Article

Multiobjective optimisation for the greener synthesis of chloromethyl ethylene carbonate by CO_2 and epichlorohydrin *via* response surface methodology

Bisi Olaniyan[†] and Basudeb Saha[†*]

[†]School of Engineering, London South Bank University, 103 Borough Road, London SE1 0AA, UK.

[*]Corresponding Author: School of Engineering, London South Bank University, 103 Borough Road, London SE1 0AA. Tel.: +44 (0)20 7815 7190; Fax: +44 (0)20 7815 7699. E-mail address: b.saha@lsbu.ac.uk (B. Saha).

Abstract: In this paper, a statistical analysis with response surface methodology (RSM) has been used to investigate and optimise process variables for the greener synthesis of chloromethyl ethylene carbonate (CMEC) by carbon dioxide (CO_2) and epichlorohydrin (ECH). Using the design expert software, a quadratic model was developed to study the interactions between four independent variables and the reaction responses. The adequacy of the model was validated by correlation between the experimental and predicted values of the responses using an Analysis of Variance (ANOVA) method. The proposed Box-Behnken Design (BBD) method suggested 29 runs for data acquisition and modelling the response surface. The optimum reaction conditions of 353 K, 11 bar CO_2 pressure and 12 h using fresh 12% (w/w) Zr/ZIF-8 catalyst loading produced 93% conversion of ECH and 68% yield of CMEC. It was concluded that the predicted and experimental values are in excellent agreement with ±1.55% and ±1.54% relative errors from experimental results for both the conversion of ECH and CMEC yield, respectively. Therefore, statistical modelling using RSM can be used as a reliable prediction technique for system optimisation for greener synthesis of chloromethyl ethylene carbonate *via* CO_2 utilisation.

Keywords: ECH, epichlorohydrin; CMEC, chloromethyl ethylene carbonate; CO_2, carbon dioxide; MOF, metal organic framework; ZIF-8, zeolitic imidazolate framework; Zr/ZIF-8, zirconium/zeolitic imidazolate framework, RSM; Response surface methodology Optimisation.

1. Introduction

Carbon dioxide (CO_2) chemistry has earned enormous interest in recent years due to its abundance and inexpensive nature. It is a nontoxic, non-flammable, easily available, and typical renewable C1 source of organic synthesis [1]. CO_2 is an important "greenhouse" gas that has drawn greater attention in line with the need for the development of green engineering and sustainable society. In this regard, the development of environmentally benign and efficient synthetic of chemical utilisation of CO_2 has been a subject of immense research in academia as evidenced by the rising number of publications in all areas of CO_2 management [2]. Although CO_2 fixation is unlikely to consume large quantities of CO_2 in the atmosphere, this measure can be regarded as a significant strategy for the development of sustainable and safe processes [3]. With the intriguing applications of organic carbonates, the use of CO_2 as a raw material to synthesize cyclic organic carbonates has gained extensive attention in chemical industries [4].

Organic carbonates are versatile compounds used as raw materials for many industrial applications including raw materials for polycarbonates and polyurethane synthesis [5], green solvents [6], gasoline [7], fuel additives [8], electrolytes in energy storage devices [9], and fine chemical intermediates for pharmaceuticals [10], automobiles [11], electronics [1] and alternative for fuels [12]. Five most important organic carbonates which have attracted significant research interest in recent years include dimethyl carbonate (DMC), diethyl carbonate (DEC), glycerol carbonate (GC), propylene carbonate (PC), and ethylene carbonate (EC) [13].

Organic carbonates has unquestionably gained popularity within the context of CO_2 utilisation campaign. However, one of the major challenges faced by chemical industries today is developing the right catalyst with the viewpoint of greener and sustainable environment . In the last decades, the use of homogeneous catalysts for the production of organic carbonates was prevalence [14]. This includes quaternary ammonium salts [9,15], ionic liquids [16], alkali metal salts [17, 18], salen Cr(III) complexes [19] [15], salen Co (III)complexes [14, 20] , and salen Mn (III) complexes [21, 22]. Some of the reasons for preference of homogeneous catalyst over solid heterogeneous catalyst include a high turnover number (TON) [23, 22], higher catalytic activity and selectivity 18]. However, homogenous catalyst have been identified with a number of environmental and economic drawbacks including high cost of catalyst production [25], rigorous separation and purification of products [23, 24], production of toxic species [27], use of co-solvent [9], problem of catalyst reusability [2] and catalyst instability at room conditions [28]. As a result of these drawbacks, extensive research efforts in catalysis have brought to spotlight the incredible advantages of heterogeneous catalyst for the synthesis of organic carbonates [29]. Heterogeneous catalysts such as metal organic framework (MOFs) catalysts offers several technical advantages such as stability, separation, handling and reuse of the catalyst and reactor design.

Heterogeneous catalysis offers several technical advantages such as stability, separation, handling and reuse of the catalyst and reactor design [22]. Metal organic framework catalyst (MOF), is a new line of heterogeneous catalyst with tremendous results for synthesis of organic carbonates. MOF catalysts, also known as multidimensional porous coordination polymers, are microporous crystalline materials with exceptional properties such as ultrahigh specific surface area, enormous pore spaces and ordered crystalline structure [30, 31]. MOFs have emerged as a suitable candidate for the cycloaddition of CO_2 and epoxide in the synthesis of organic carbonate due to their heterogeneity and reusability requirements [32]. The development of an efficient and stable Zr/ZIF-8 catalyst for the synthesis of chloromethyl ethylene carbonate (CMEC) from epichlorohydrin (ECH) and CO_2 is a promising greener technology for CO_2 utilisation. Incorporating zirconium into ZIF-8 has undoubtedly increased ZIF-8 stability as well as the catalytic performance of Zr/ZIF-8 during the series of experiments.

Within the context of Chemical Engineering, low product yields have been attributed to a number of factors including the use of unsuitable choice of catalyst [33], problems achieving the right optimum reaction conditions [27] and inappropriate application of other input parameters [34]. In recent years, optimising system variables to improve product yields have been the focus of many different fields of research. Response surface methodology (RSM) is a collection of statistical and

mathematical techniques based on the multivariate non-linear model for optimising processes [35]. RSM has received considerable interests in many industrial processes in an attempt to construct empirical models able to correlate the statistical relationships (if any) between a set of variables making up an industrial system [34]. Saada et al. [27] and Onyenkeadi et al. [36] have successfully modelled and optimised the synthesis of organic carbonates with five independent variables at 3-levels (3^5) factorial design. Their results have been validated using regression analysis.

Several authors including AboElazayem et al. [37] and Saada et al. [27], have criticised the traditional 'trial-and-error'' optimisation methods and ''one-factor-at-a-time'' (OFAT) as time-consuming and considered quite expensive due to a large number of samples and experimental trials involved. Another drawbacks identified with traditional optimisation methods is low overall efficiency [38]. Sadeghi and Sharifnia [39], describes OFAT as a method that excludes the interactive effects among the variables and does not express the complete effects of the parameters on the process. In order to overcome these drawbacks, Yu and He [40] suggested multivariate statistical techniques, which are full three-level factorial designs: Box-Behnken designs, central composite designs and Doehlert designs.

A multivariate optimisation technique is a statistical tool for analysing complex non-linear processes. This is especially useful when interactions are not known or optimal process parameters are to be determined in order to make a process more robust [41]. It is cost-effective as fewer experimental trials are required, high computational efficiency [39] and it requires very little or no human experience to obtain an accurate and satisfactory results [27]. Therefore, the systematic application of RSM optimisation for the catalytic conversion of epichlorohydrin (ECH) and carbon dioxide (CO_2) to chloromethyl ethylene carbonate (CMEC) can be regarded as an innovative way of CO_2 utilization

2. **Experimental Methods**

2.1. Chemicals and materials

Acetone (99%), chloromethyl ethylene carbonate (99 %), epichlorohydrin (purity; 99%), zinc nitrate hexahydrate ($Zn(NO_3)_2{\cdot}6H_2O$ (purity; 99%), dimethylformamide (purity; 99%) and zirconium (IV) oxynitrate hydrate ($ZrO(NO_3)_2{\cdot}6H_2O$, 99.99%) were purchased from Sigma-Aldrich Co. LLC. Methanol (99%) and *n*-pentane 99.8%) were both procured from Fisher Scientific UK Ltd. ZIF-8 catalyst was purchased from Sigma-Aldrich Co. LLC under the trademark of Basolite Z1200. All chemicals and catalysts were used without further purification or pre-treatment

2.2 Catalysts preparation

Zirconium-doped ZIF-8 (Zr/ZIF-8) was synthesised according to a method, which was previously described elsewhere [42,43]. Briefly, 8 mmol of zinc nitrate hexahydrate ($Zn(NO_3)_2{\cdot}6H_2O$, purity 99.99%) and zirconium (IV) oxynitrate hydrate ($ZrO(NO_3)_2{\cdot}6H_2O$, purity 99.99%) solutions in a stoichiometric ratio of Zn: Zr =9:1 were dissolved in 6.2 mmol of methanol. A separate solution of 14.2 mmol of 2-methylimidazole and 600 mml of methanol was prepared in another flask which was added by dropwise addition to the Zr-Zn based solution. The mixture conducted in an ambient temperature under nitrogen gas flow was vigorously stirred for 6 hrs. The crystals were collected and separated by centrifugation at 300 rpm for 30 min. The solution was washed thoroughly with methanol three times and then dried at room temperature. The crystals were left to dry overnight at 373 K. The greyish-white powders of Zr-ZIF-8 sample were further washed with DMF for 24 h in order to remove any excess of an unreacted organic linker. The solution was then heated at a temperature of 373 K in order to activate it. The sample was allowed to cool down to room temperature naturally before been capped in a vial and refrigerated, which was ready for use in catalytic reactions.

2.3. Proposed reaction mechanism and reaction pathways

On the basis of our experimental results and theoretical understanding, we proposed a plausible reaction mechanism for the coupling reaction of ECH and CO_2. Figure 1 shows the reaction mechansim was initiated by coordination of ECH with Lewis acid site Zn^{2+} to form the adduct of zinc-epoxide complex, then nucleophilic interaction on the electrophilic carbon of CO_2 (step 1). At the same time, the acidic sites (unsaturated coordinative Zn or structural defects) of Zr/ZIF-8 interact with the oxygen atom of an epoxide (step 2). The activated CO_2 attacks the less sterically hindered carbon atom of epoxide, which results in the epoxide ring-opening (step 3). Finally, the ring-closure step takes place between the O−anion and carbon atom in the intermediates to produce CMEC (step 4). Figure 2 shows the reaction pathways 1, 2 and 3 with some by-products. The decline in selectivity and CMEC yield was expected because the gas chromatography mass spectroscopy (GC-MS) analysis of the samples shows that 17.3% of 3-chloropropane 1,2-diol and 14.1% 2,5-bis (chloromethyl)-1,4-dioxane (by-products) have been formed at 353 K. Similar by-products and results have been reported by Mousavi et al. [65]. This may explain in part why a drop in selectivity and yield of CMEC was recorded.

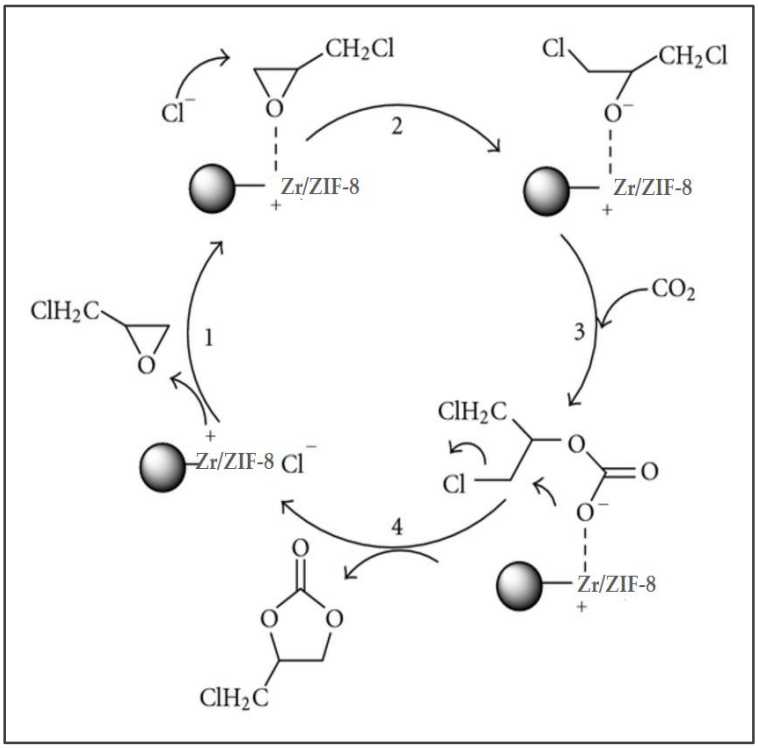

Figure 1. Proposed reaction mechanism for cycloaddition reaction of ECH and CO_2

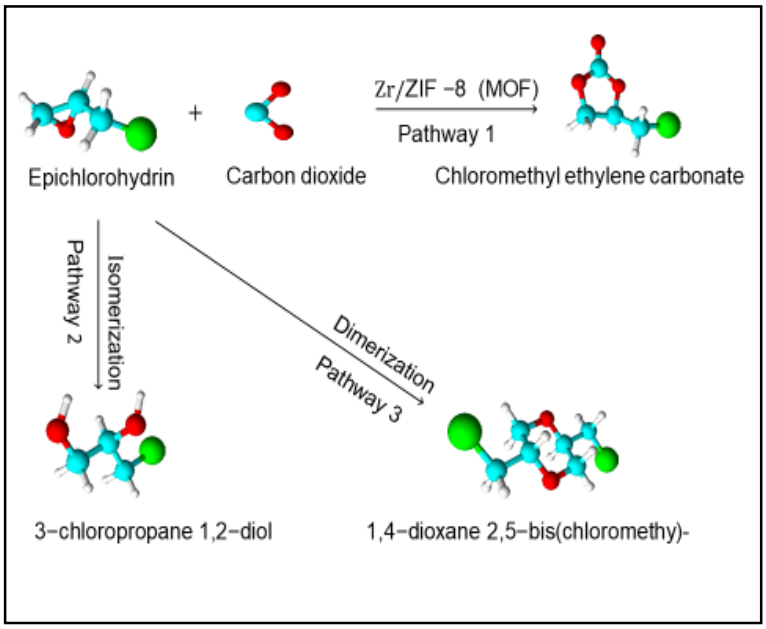

Figure 2. Reaction pathways for cycloaddition reaction of ECH and CO_2

2.4 One-factor-at-a-time (OFAT) analysis

OFAT analysis was developed to determine the preliminary effective range of the selected parameters for statistical analysis. The effect of 4-single factors (temperature, pressure, reaction time and catalyst loading) were evaluated for the synthesis of chloromethyl ethylene carbonate. The OFAT analysis investigated all the four parameters in the following range: reaction temperature K (313, 323, 333, 343, 353, 363, 373); pressure (bar) (4, 6, 8, 10, 12, 14, 16); catalyst loading (%) (w/w) (5, 7.5, 10, 12.5, 15); reaction time (h) (4, 6, 8, 10, 12, 14, 16).

2.5 Experimental design

Based on the OFAT results, a 3-level, 4-factor (3^4) factorial design with 29 runs of experiments were suggested for this study in order to determine the responses (conversion and yield). In this design, all the four factors were varied simultaneously over a set of experimental runs. To avoid bias, the suggested set of experiments were carried out randomly and the four factors: temperature, pressure, catalyst loading and reaction time have been labelled as x_1, x_2, x_3 *and* x_4 respectively as shown in Table 1. The variables and their coded and uncoded values are presented with each levels and range as given below in Table 1 (i.e. −1, 0, 1).

Table 1. Experimental design variables and their coded levels

Variables	**Code**	**Range and Levels**		
		-1	0	+1
Temperature (K)	x_1	313	353	373
Pressure (bar)	x_2	4	8	16
Catalyst loading (w/w)	x_3	5	7	15
Time (h)	x_4	4	8	16

178 The total number of experiments (N) is given by Equation (1)

179

180 $$N = k^2 + K + C_p \quad (1)$$

181

182 Where, k is the number of independent variables, Cp is the replicate number of the centre point.

183

184 **Table 2:** Experimental design matrix with the actual and predicted responses

Run	T x_1 (K)	P x_2 (bar)	t x_3 (h)	Catalyst loading x_4 (w/w)	Actual ECH conv. (%)	Predicted ECH conv. (%)	Actual CMEC yield (%)	Predicted CMEC yield (%)
1	313	4	8	7	42	46.33	16	14.63
2	353	8	16	5	67	68.17	33	32.29
3	353	8	8	7	84	84.00	64	64.00
4	313	16	16	7	58	59.88	29	31.67
5	353	8	8	7	84	84.00	64	64.00
6	353	8	4	5	52	55.67	26	26.46
7	353	4	16	7	75	72.96	40	41.04
8	313	8	8	5	54	55.79	23	24.88
9	353	16	16	7	93	93.29	65	66.04
10	313	8	8	15	58	56.46	31	30.38
11	353	16	8	5	86	81.21	36	35.00
12	373	16	8	7	86	81.67	45	46.13
13	373	4	8	15	75	82.33	54	57.63
14	353	16	8	15	88	91.38	68	68.00
15	373	8	4	7	68	62.38	38	33.33
16	353	8	8	7	84	84.00	64	64.00
17	373	8	16	15	90	85.38	64	60.67
18	373	16	8	5	54	59.29	26	28.88
19	313	16	8	7	90	82.67	55	51.13
20	373	8	8	15	86	87.96	64	64.38
21	353	4	4	7	68	64.46	35	36.21
22	353	8	8	15	84	84.00	64	64.00
23	353	8	8	7	84	84.00	64	64.00
24	353	16	4	15	70	75.79	35	36.21
25	313	8	4	15	52	52.88	23	24.33
26	353	8	16	15	89	85.33	65	64.29
27	353	4	8	5	66	58.88	37	33.50
28	353	4	8	15	77	78.04	44	43.00
29	373	8	4	15	69	67.83	35	35.46

185

2.6. Statistical analysis

The empirical mathematical model showing the effect of the independent variables x_1, x_2, x_3 and x_4 on the predicted response Y was investigated using the second order polynomial regression equation with backward elimination.

A quadratic equation derived using RSM for the model is shown using Eq. 2:

$$Y = b_o + \sum_{i=1}^{n} b_i x_i + \sum_{i=1}^{n} b_{ii} x_i^2 + \sum_{i=1}^{n-1} \sum_{j>1}^{n} b_{ij}\, x_i x_j + \quad \mathcal{E} \qquad (2)$$

where Y is the predicted response, x_i and x_j are the independent variables in coded levels ($i \neq j$), b_i, b_{ii}, and b_{ij} are the coefficients for linear, quadratic and interaction effects, respectively, b_0 is the model coefficient constant, n is the number of factors, and $\mathcal{E}$ is the model random error [46].

The adequacy of the predicted models was validated by a number of statistical tools such as correlation coefficient (R^2), adjusted coefficient of determination (R^2_{adj}) and the predicted coefficient of determination (R^2_{pred}). The statistical significance of the predicted model was analysed by (ANOVA) using a regression coefficient by conducting the Fisher's F-test at 95% confidence level [27]. Design Expert 11 software (Stat- Ease Inc., Minneapolis, MN, USA) was used for the design of experiment, regression and graphical analysis. Statistical significance of the results have been presented by $p < 0.05$ and mean ± SE. The fit quality of the polynomial equation has been proved by R^2.

2.7. Experimental procedures

In a typical cycloaddition reaction, chloromethyl ethylene carbonate (CMEC) was synthesised from epichlorohydrin (ECH) and carbon dioxide (CO_2) in a solvent free and co-catalyst free conditions. A 25 mL stainless steel autoclave reactor equipped with a stirrer, thermocouple, heating mantle and controller was initially charged with the required amount of limiting reactant ECH and a known amount of Zr/ZIF catalyst. The reactor was then heated to a specific temperature and continuously stirred. When the desired reaction temperature was reached, a known amount of liquid CO_2 was injected to the reactor *via* SCF pump at an assumed t=0. The reaction mixture was left stirring and monitored for a set period of time.

After the reaction was completed, the reactor was cooled down to room temperature using an ice bath, depressurized and then the reaction mixture was filtered. The catalyst was separated, washed with acetone and dried in a vacuum oven. The product obtained from the filtered reaction mixture was then analysed using gas chromatography (GC).

3. Results and Discussion

3.1 Analysis of variance (ANOVA)

An analysis of variance (ANOVA) was performed using the Design Expert software in order to investigate the fitness and significance of the model for each regression coefficient. The empirical analysis of RSM model used to correlate the interactive relationship between the controlling factors (x_1, x_2, x_3 *and* x_4) and the predicted response Y (conversion of ECH and yield of CMEC) are shown in Table 2 above. The results of the experimental trials at various process conditions show the range of the responses from 42 to 93% of ECH conversion and 16 to 68% of CMEC yield. This trend is consistent with the results published by Saada et al. [27] and Onyenkeadi et al. [36]. The predicted values sufficiently correlate with the observed values and fit the RSM model design for this study. The best fitting model was established by a regression analysis using Design Expert software. Fitting

of the data to various models (linear, two factors interactions (2FI), quadratic and cubic polynomials) and their following analysis of variance [ANOVA].

3.2 Development of regression model

In this study, the purpose of using the RSM was to generate a statistical model that demonstrate mutual interaction between the responses and the effective variables. Through the experimental matrix generated in a randomised run of experiments, the obtained responses are given using second order polynomial regression equation with backward elimination as shown below. The equations show the empirical relationship between the conversion of ECH and the yield of CMEC and the experimental factors in coded forms.

$$Y_1 = 84.15 + 8.75\,x_1 + 8.86\,x_2 + 7.22\,x_3 + 7.500x_4 - 9.005\,x_1x_2 + 7.25\,x_1x_3 + 4.15\,x_1x_4 - 2.150\,x_2x_3 + 2.10\,x_2x_4 + 1.10\,x_3x_4 - 11.45\,x_1^2 + 0.80x_2^2 - 7.10\,x_3^2 - 7.30\,x_4^2 \quad (3)$$

$$Y_2 = 64.15 + 9.10\,x_1 + 6.30\,x_2 + 10.30\,x_3 + 8.70\,x_4 - 12.15\,x_1x_2 + 7.25\,x_1x_3 + 5.25\,x_1x_4 + 5.40\,x_2x_3 + 6.30\,x_2x_4 + 5.60\,x_3x_4 - 14.40\,x_1^2 - 7.55\,x_2^2 - 12.75\,x_3^2 - 12.15x_4^2 \quad (4)$$

Y_1 and Y_2 are the response variables: ECH conversion and CMEC yield. The independent variables are x_1, x_2, x_3 *and* $x_4$re which are reaction temperature, pressure, catalyst loading and reaction time, respectively. The results of interaction effects between the independent variables were deduced as follows: (temperature-pressure; x_1x_2, temperature-catalyst loading; x_1x_3, temperature-reaction time; x_1x_4, pressure-catalyst loading; x_2x_3, pressure–time; x_2x_4 and catalyst loading –reaction time; x_3x_4). Finally, the excess of each independent variable was represented as follows: (temperature-temperature; x_1^2, pressure-pressure; x_2^2, catalyst loading-catalyst loading; x_3^2 and reaction time – reaction time; x_4^2).

Table 3. Analysis of variance (ANOVA) of developed model for ECH conversion

Source	Sum of square	Diff.	Mean Square	F Value	p-value	Significance
Model	5014.09	14	362.01	11.21	< 0.0001	HS
x_1-temperature	827.75	1	827.75	26.02	0.0001	HS
x_2-pressure	854.08	1	854.08	27.10	< 0.0001	HS
x_3-catalyst loading	871.33	1	871.33	18.68	0.0006	HS
x_4-reaction time	619.00	1	619.00	21.58	0.0005	HS
x_1x_2	308.25	1	308.25	9.44	0.0060	HS
x_1x_3	177.00	1	177.00	4.98	0.0283	S
x_1x_4	58.00	1	58.00	1.95	0.1842	NS
x_2x_3	18.25	1	18.25	0.62	0.4451	NS
x_2x_4	38.25	1	38.25	1.29	0.2754	NS
x_3x_4	5.15	1	5.15	0.19	0.6691	NS
x_1^2	789.39	1	789.39	25.73	0.0001	HS
x_2^2	4.16	1	4.16	0.15	0.7030	NS
x_3^2	353.82	1	353.82	11.13	0.0049	S

x_4^2	336.95	1	336.95	9.40	0.0061	S
Residual	448.08	14	34.86			
Lack of Fit	448.08	10	44.81	0.44	0.56	NS
Pure Error	0.000	4	0.000			
Cor Total	5553.17	28				

S: significant.
NS: not significant.
HS: highly significant

Table 4. Analysis of variance (ANOVA) of developed model for CMEC yield

	Sum of square	difference	Mean Square	F Value	p-value	Significance
Model	7335.55	14	431.90	68.68	< 0.0001	HS
x_1-temperature	1023.00	1	1023.00	139.85	< 0.0001	HS
x_2-pressure	468.75	1	468.75	60.53	< 0.0001	HS
x_3-catalyst loading	1260.75	1	1260.75	162.80	< 0.0001	HS
x_4-time	901.33	1	901.33	116.39	< 0.0001	HS
x_1x_2	576.00	1	576.00	74.38	< 0.0001	HS
x_1x_3	225.00	1	225.00	29.05	< 0.0001	HS
x_1x_4	100.00	1	100.00	12.91	0.0029	HS
x_2x_3	119.00	1	119.00	15.62	0.0014	HS
x_2x_4	146.25	1	146.25	20.18	0.0005	HS
x_3x_4	128.25	1	128.25	17.08	0.0010	HS
x_1^2	1258.78	1	1258.78	176.11	< 0.0001	HS
x_2^2	347.29	1	347.29	42.52	< 0.0001	HS
x_3^2	897.34	1	897.34	128.27	< 0.0001	HS
x_4^2	897.05	1	897.05	120.62	< 0.0001	HS
Residual	104.24	14	7.87			
Lack of Fit	104.24	10	10.43	1.35	0.325	NS
Pure Error	0.000	4	0.000			
Cor Total	7444.79	28				

S: significant.
NS: not significant.
HS: highly significant

3.3. Statistical analysis of regression model

The response model calculated for this study has demonstrated a high degree of accuracy with an R^2 of 0.9973 and an R^2_{adj} of 0.9954 at a confidence level of 95 %. This agrees well with the result of [37] where the determination coefficient values, R^2 and R^2_{adj}, for the reliability of the model fitting,

were calculated to be 0.9932 and 0.9658, respectively. Mäkelä et al. [47], also suggested that a good model fit should yield an R^2 of at least 0.8. Furthermore, the values of R^2 and R^2_{adj} are close to1.0. This demonstrates that a mutual correlation exists between the experimental and the predicted values. Therefore, the statistical significance of the second-order polynomial equation for this design shows that the regression model is statistically significant ($P<0.0001$) and the lack of fit test is non-significant ($p>0.05$) relative to the pure error.

The following assumptions have been used to conclude the statistical adequacy checking of the model based on the ANOVA results. The first assumption is the similarity between the predicted and actual data of the two models as shown in Figure 3. This demonstrated that the variations between Figures 3a and 3b are statistically non-significant (NS) and the predicted model can be said to show a high level of accuracy and the adequacy. Another assumption is the normality of the residuals. The plot of residuals has been investigated using normal plot where most of the points approximately form a straight line as shown in Figures 4a and 4b. This shows that residuals for both ECH conversion and CMEC yield are in normal distribution. This assumption is consistent with the report of Mäkelä [47]. Thirdly, the randomisation of the residuals have also been assessed using a plot between the residuals *versus* predicted responses. The random distribution in Figure 5 shows lack of clear structure with a normal distribution at zero mean and variance [48]. It can be observed in Figures 5a and 5b that points above and below the diagonal line show areas of over or under prediction with no definite structure.

3.4. Model Fitting and adequacy checking

In order to verify the model for fitting and adequacy test at 95% confidence level, it was necessary to apply analysis of variance (ANOVA). As shown in Tables 3 and 4, the ANOVA results indicated a good model fit with the model F-value is 0.44 (Table 3) and the probability > F of less than 0.0001 implied that this model was significant. The lack of fit test (non-significant: $p>0.05$) was also considered a good statistical indicator for the model adequacy checking as it relates the residual error to the pure error from the replica design point [49]. As indicated in ANOVA Tables 3 and 4, the conversion of ECH and CMEC yield was significantly ($p<0.05$) influenced by the interactive and quadratic effects of all the independent variables.

3.5 Response surface plots analysis

After the regression models had been built and model adequacy checking was tested, 3D response surface plots and their corresponding 2D contour plots were drawn for a model equation. Different shapes of the contour plots indicate different levels of interaction between two variables. For example, an oval plot represents significant interactions between the two selected variables while a circular plot means otherwise [50]. According to Rabiee et al. [51], 3D response surface promotes understanding of system behaviour. It is also significant in recognising the characters of response surface [52].

4.0. Effect of one factor at a time experiments on responses (OFAT)

The effects of individual reaction variables (temperature, pressure, time and catalyst loading) and their interactions on reaction responses (conversion and yield) have been investigated using the 3D-surface and 2D-contour plots generated from the predicted quadratic model as evidenced in Figures 6 to 9. The experiments have been carried out by varying one reaction parameter at a time while keeping other parameters constant at the following reaction conditions: reaction temperature 353 K, CO_2 pressure 11 bar, reaction time 12 h, catalyst loading 12% (w/w).

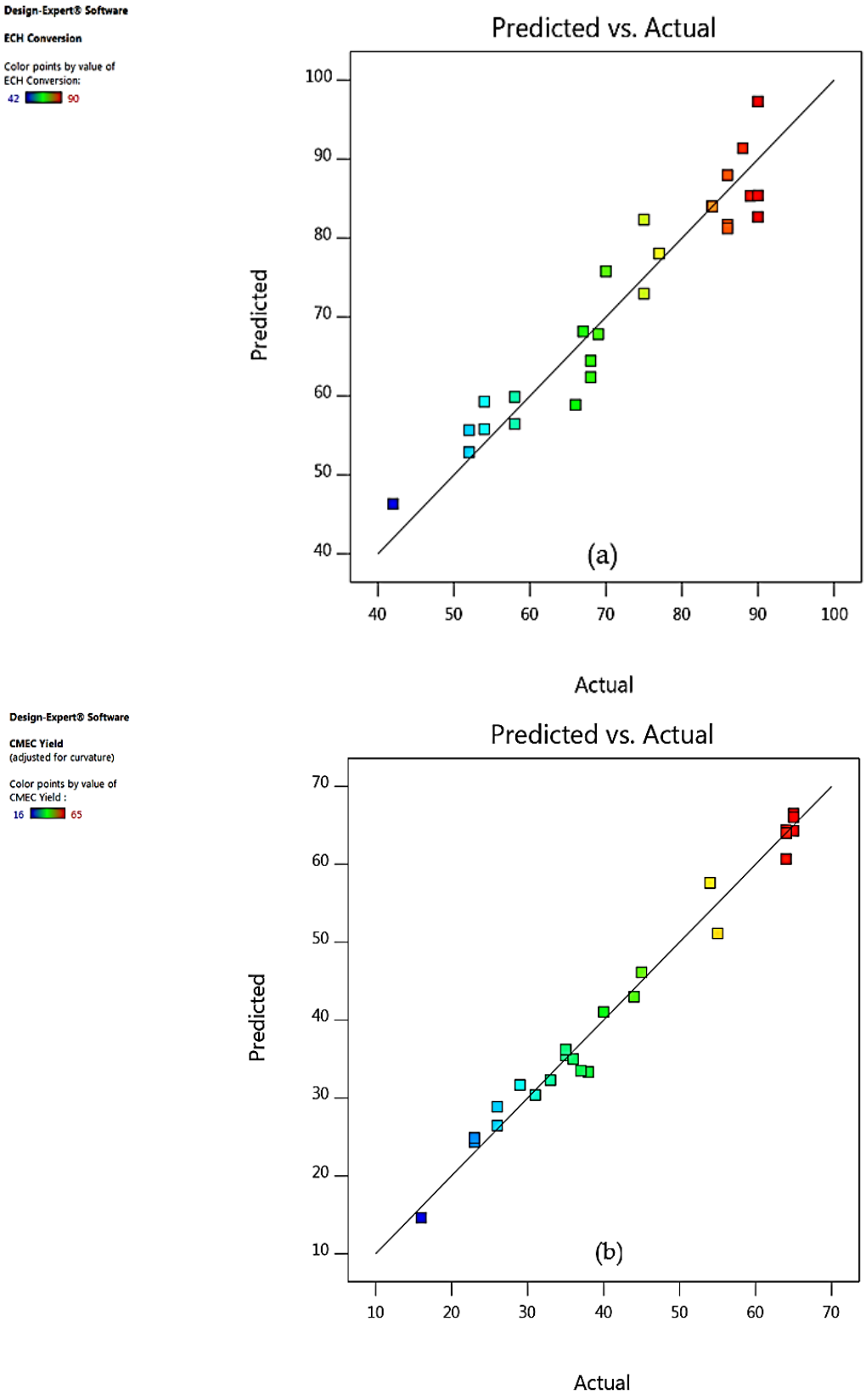

Figure 3. Predicted *versus* actual values models for (a) ECH conversion and (b) CMEC yield.

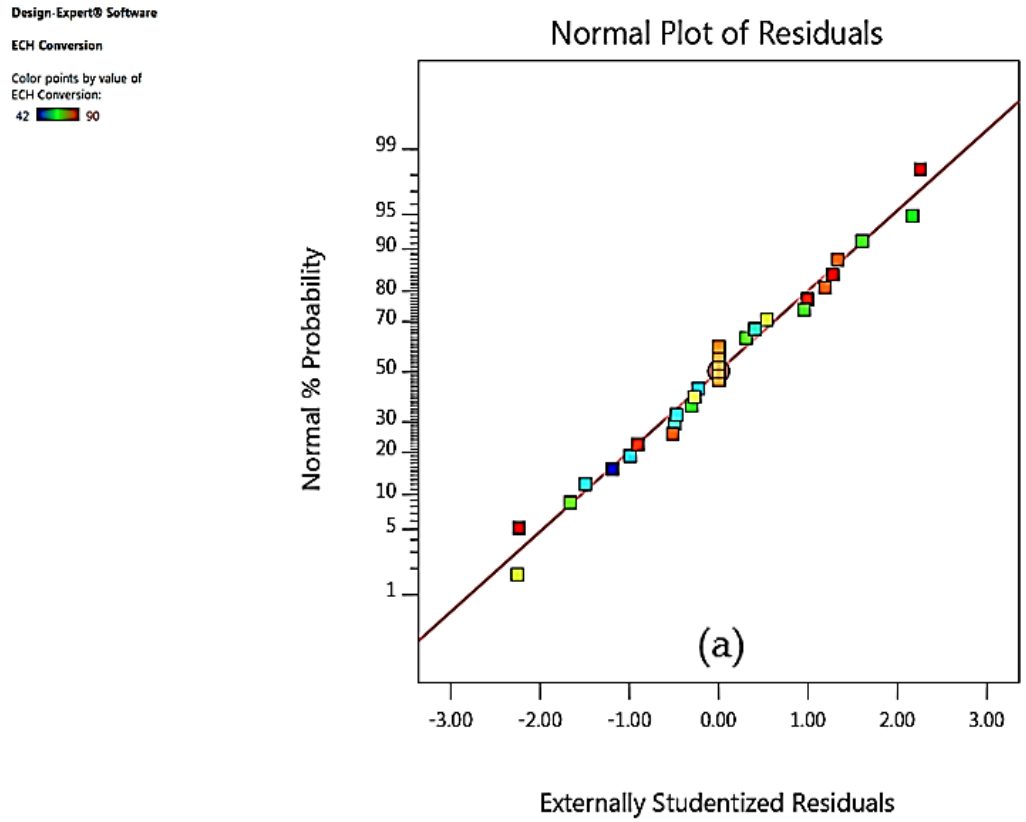

328

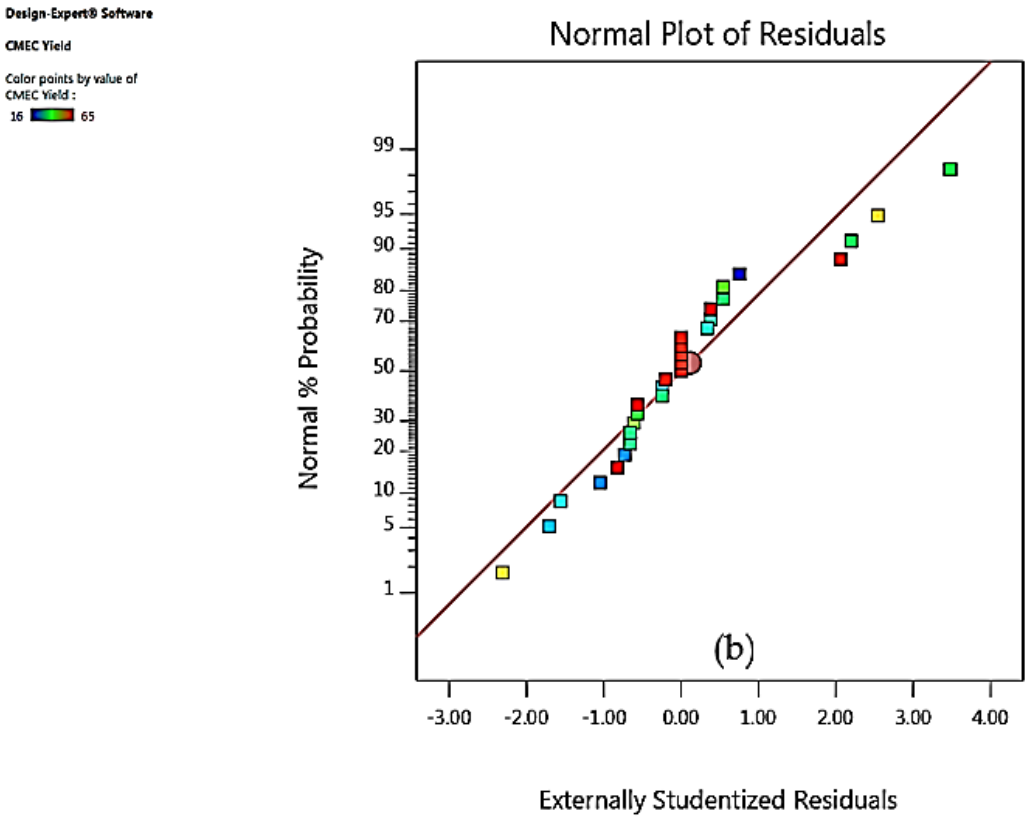

329

330 **Figure 4**. Normal plot of residuals for (a) ECH conversion and (b) CMEC yield.

331

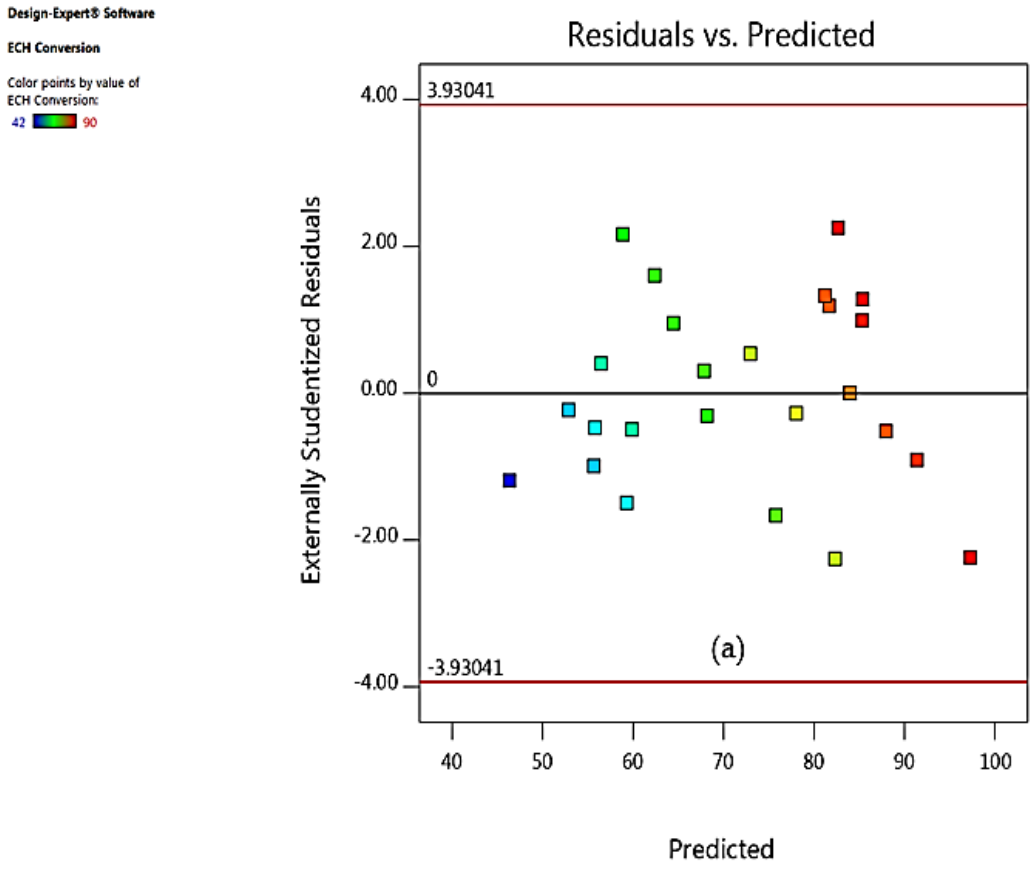

332

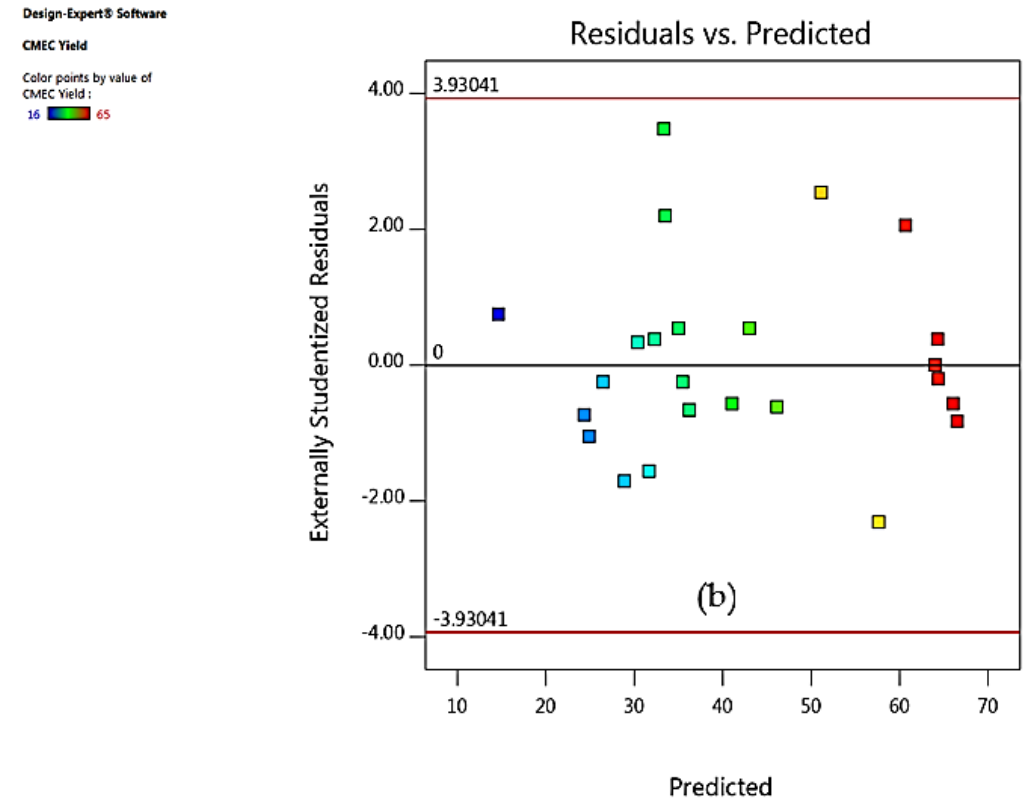

333

334 **Figure 5**. The plot of residuals *versus* predicted response for (a) ECH conversion and (b) CMEC
335 yield.

4.1.1 Effect of reaction temperature

To a significant extent, it is largely agreed that a directly proportional relationship exists between temperature and CMEC yield as shown in the results of ANOVA in Table 4. The influence of reaction temperature on CMEC yield has been investigated by varying temperature over the range of 323 K to 373 K. As evidenced in Figure 6, CMEC yield increased steadily from 40% to 68% as temperature increased from 323 K to 353 K. However, a gradual decrease in CMEC yield was observed at higher temperature values beyond 353 K. This may be due to the formation of diols and dimers of epichlorohydrin above optimum temperature [53]. Saada et al. [27] explained that higher reaction temperatures caused a shift in the equilibrium to the reactant side and resulted in a reduced DMC yield. The same temperature effect was also reported by Kilic et al. [54], they have observed that as they increased the reaction temperature from 348 K to 373 K (while keeping other variables constant), there was a corresponding increase in ECHC yield from 65.8% to 97.0%. However, further increase in temperature beyond 373 K, caused a slight decrease both in the ECHC yield and catalyst selectivity.

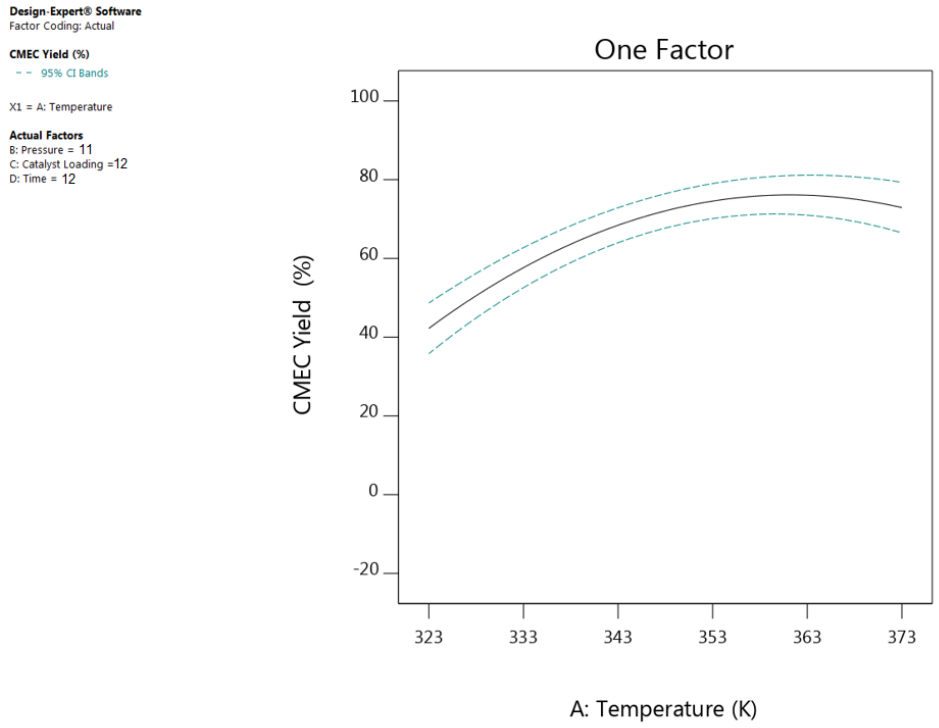

Figure 6. The plot showing the effect reaction of temperature on CMEC yield

4.1.2. Effect of CO_2 pressure

ANOVA Table 4 demonstrates the dependence of CO_2 pressure on CMEC yield, since CO_2 acts both as reactant and reaction medium simultaneously [55]. As indicated in Figure. 7, when CO_2 pressure was increased from 8 to 11 bar, the CMEC yield also increased from 50% to 68%. Conversely, with the CO_2 pressure of 11.5 bar, a 59% CMEC yield was recorded indicating a declining effect. Zhong et al. [56] demonstrated the effect of variation in CO_2 pressure on organic carbonates. They have enhanced more propylene carbonate (PC) yield when CO_2 pressure was increased from 1 MPa to 3 MPa. However, when CO_2 pressure was further increased to 4MPa, they observed that the concentration of propylene oxide (PO) in gas phase had decreased as a result of dilution by CO_2 and consequently resulted in a reduced PC yield. It is therefore concluded that the optimum CO_2 pressure based on OFAT analysis for this set of experiments was 11 bar of CO_2 pressure.

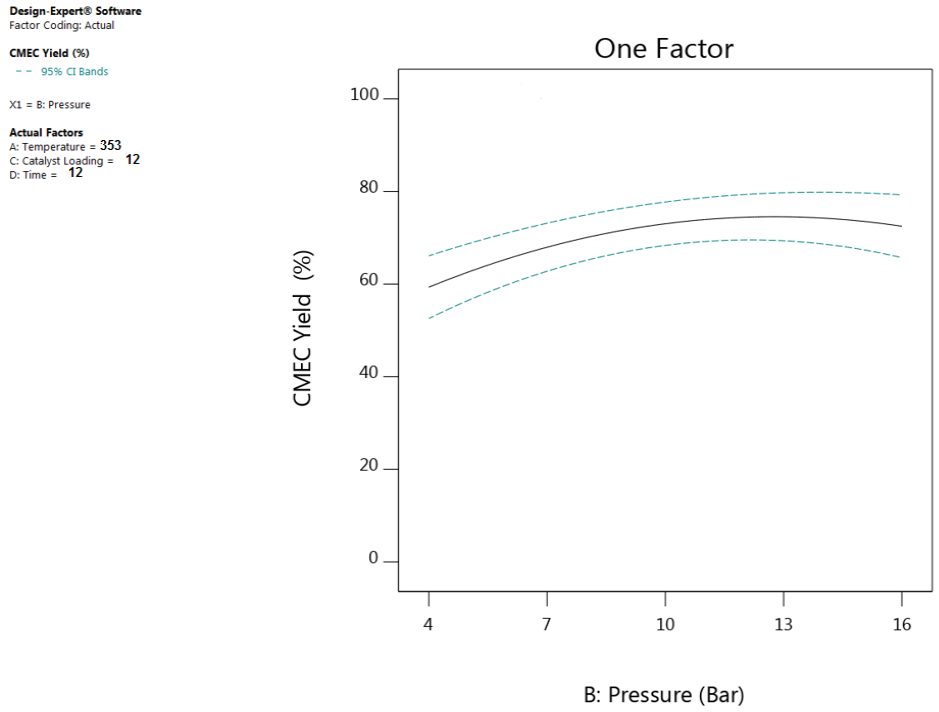

Figure. 7. The plot showing the effect of CO_2 pressure on CMEC yield

4.1.3 Effect of reaction time

Reaction time is one of the crucial factors in a catalytic reaction. Figure 8 shows a direct proportionality effect between reaction time and the CMEC yield; the yield increased gradually as reaction time increased until it reaches 68% in 12h. Further increase in reaction time beyond 12 h, resulted in a continuous decline in CMEC yield as shown in Figure 8. This could be as a result of formation of polymerised CMEC caused by prolonged reaction time [8]. A similar phenomenon was also reported by Onyenkeadi et al.[36], where increasing in reaction time from 8 to 16 h was directly proportional to butylene carbonate (BC) yield. However, prolonged reaction time beyond this time resulted in decrease in BC yield.

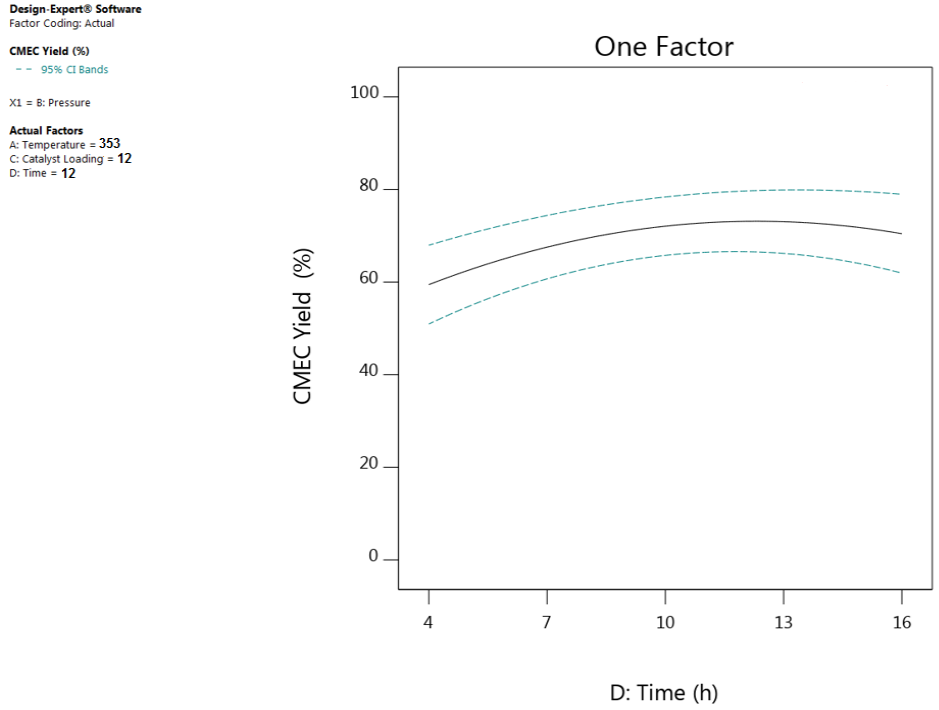

Figure. 8. The plot showing the effect of reaction time on CMEC yield

4.1.4 Effect of catalyst loading

The effect of catalyst loading on CMEC yield was investigated by varying Zr/ZIF-8 loading from 5 to 15% (w/w). As shown in Figure 9, it can be observed that as catalyst loading was increased, CMEC yield also increased proportionally from 42% reaching a maximum of 68% at 12% (w/w) catalyst loading. It was then decreased progressively when the amount of catalyst was further increased to 13% (w/w), indicating that optimum catalyst loading had been exceeded. It would be expected that the number of active sites available for the reaction of ECH and CO_2 would increase as catalyst loading increases [57]. However, Han et al. [58] argued that an excessive increase in catalyst loading tends to provoke formation of undesirable side-products (in their experiment, a by-product of diglyceride (GDL) or triglyceride (GTL) was formed), thereby causing a drop in glycerol monolaurate (GML) selectivity as they increased the amount of catalyst beyond 2% (w/w). Similarly, in the present work, increase in the amount of catalyst loading beyond the optimum level was unfavourable to the reactive system resulting in a reduced CMEC yield. Therefore, the optimum catalyst loading for this reactive system is 12% at a reaction temperature of 353 K for 12 h at 11 bar of CO_2 pressure.

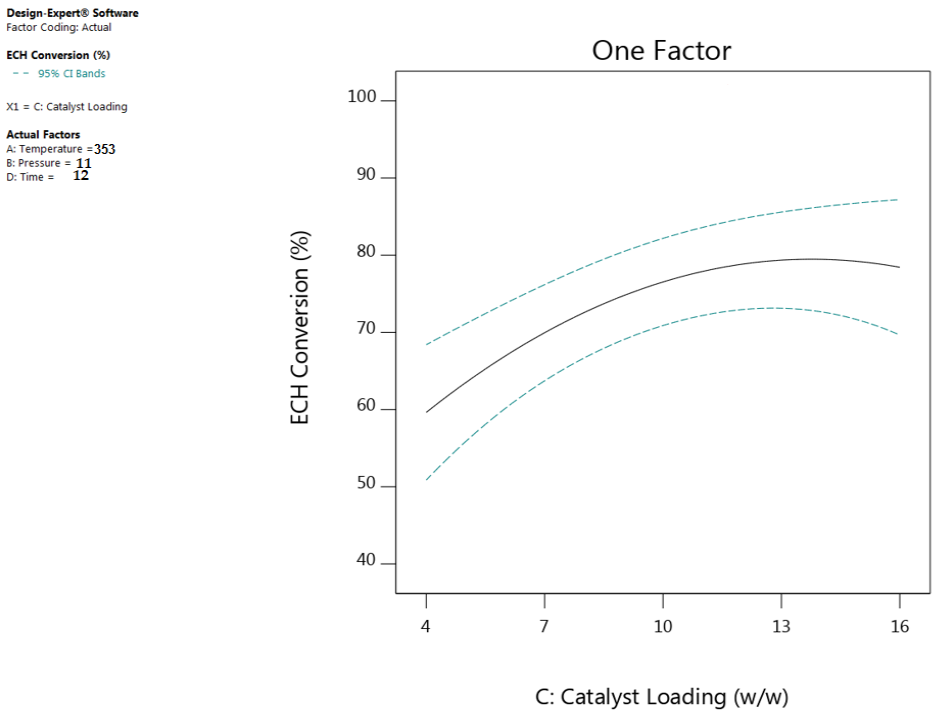

Figure. 9. The plot showing the effect of catalyst loading on CMEC yield

5.0 Interactive effect of process variables on responses

The interaction effect of each pair of reaction variables have been investigated using ANOVA results, 3D surface and 2D contour plots. The interaction effect of some process variables on ECH conversion and CMEC yield produce different effect at different levels of other variables. Therefore, 3D plots have played a crucial role in making accurate predictions about process optimisation [59]. From ANOVA Table (3 and 4), it can be observed that all the four reaction parameters are deemed significant and can affect the process response tremendously at different levels of interaction. Hence, the interactive effect of process variables has a direct influence on the system optimisation. The interaction effect between a pair of variables would be negligible if the contour plot of the response surface is circular. Conversely, the interactions effect would be significant if the contour plot is elliptical [60]. Therefore, instead of studying single variable (as in conventional method) the interactions were investigated which is significant for a comprehensive optimisation study

5.1 Interactive effect of temperature and pressure

As depicted in Figure. 10 and the ANOVA Tables 3 and 4, the interaction effect of reaction temperature and CO_2 pressure has played significant roles in both ECH conversion and CMEC yield (while keeping reaction time and catalyst loading at their optimum: 12 h and 12 % (w/w) respectively). At lower reaction temperature (e.g. at 323 K), increase in the CO_2 pressure from 4 to 16 bar increases the CMEC yield from 47 to 68%. However, at higher reaction temperature beyond 353 K showed a negative effect on CMEC yield (Figure. 10a), this could possibly be as a result of formation of by-products at elevated temperature as indicated in the reaction mechanism (Figure 1). Furthermore, at a different level of interaction between temperature and pressure (e.g. from 358 K to 373 K and 13-16 bar), a notable effect was also recorded where there was a gradual decline in the CMEC yield indicating optimum condition had been exceeded. This shows that variation in reaction temperature had a negative effect on both responses at higher values. Therefore, the temperature-

pressure relationship has significant effect on process responses. Similarly, the elliptical shape of the 2D contour plot in Figure. 10b exemplifies a mutual interactive effect of the reaction variables on responses.

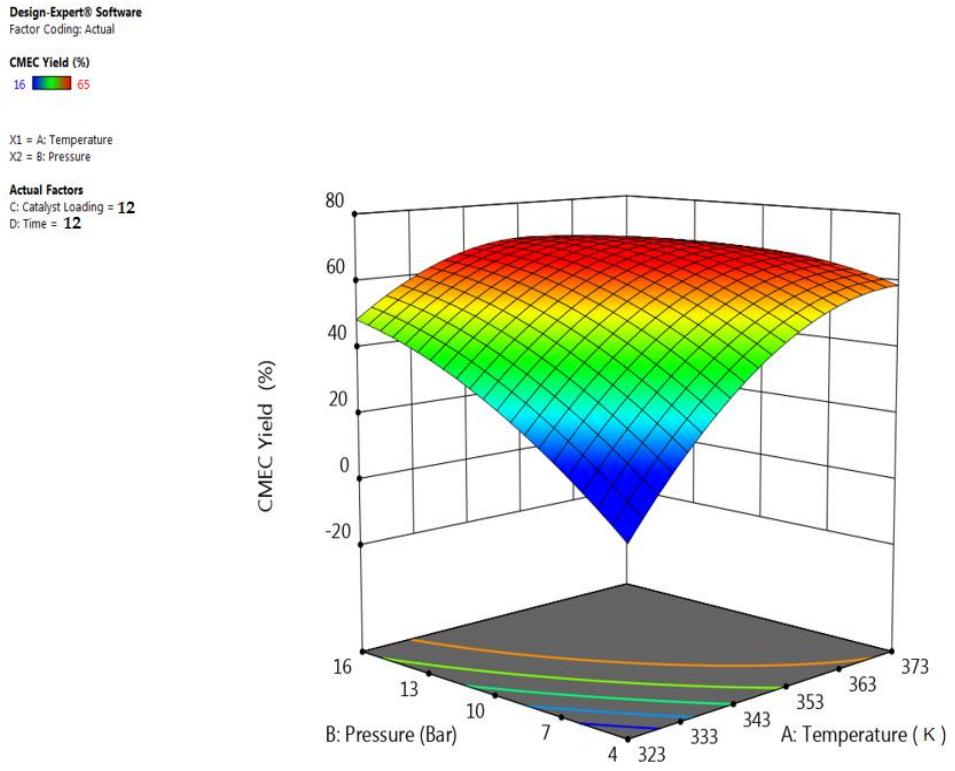

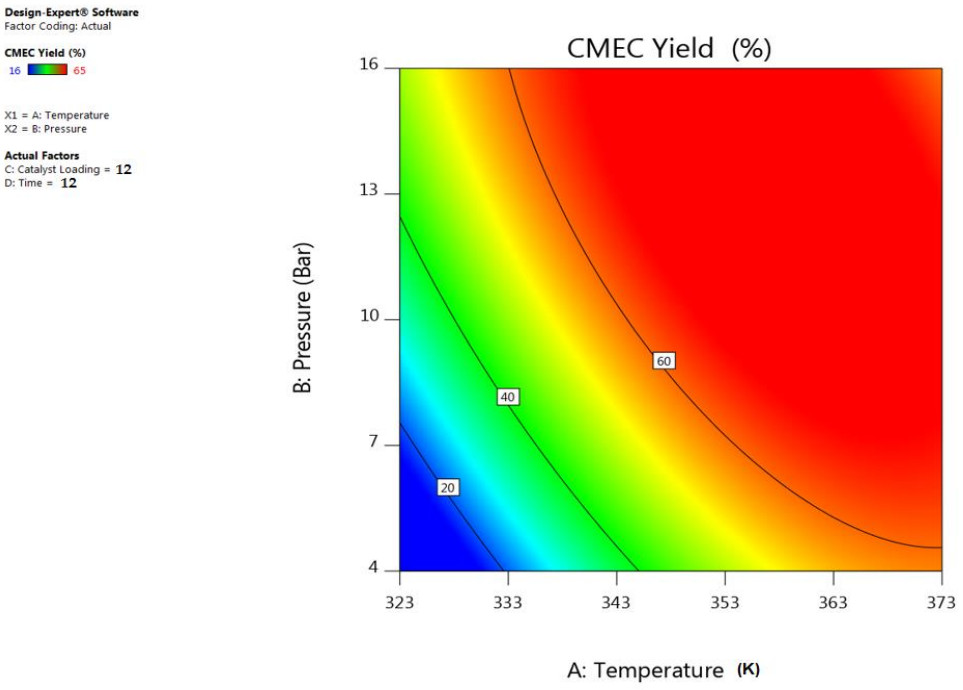

Figure 10. (a) 3D response surface and (b) contour plot of reaction temperature and pressure *versus* CMEC yield

5.2. Interactive effect of temperature and time

Figure 11 illustrated the interaction effect of reaction time and temperature on CMEC yield (while keeping other two variables at their optimum: catalyst loading: 12 % (w/w), CO_2 pressure: 11 bar). The surface plot suggested that the CMEC yield was highest (68%) at a reaction time of 12 h and temperature of 353 K indicating that an increase in the reaction temperature from 313 K to 353 K favours ECH conversion and consequently enhancing CMEC yield as shown in Figure 11a. However, increase in reaction temperature beyond 353 K at 12 h of reaction time was unfavourable to the reactive system causing a marginal drop in CMEC yield from 68% to 65%. Onyenkeadi et al. [9] reported that formation of oligomers and isomers are possible at extended reaction time at higher temperature. Product quality and stability may also be affected due to chemical degradation or losses by thermal decomposition at higher reaction temperature [8]. Response surface and contour plots of Figure 11 clearly shows that CMEC yield had a linear effect with increasing reaction temperature until the optimum condition was achieved. This phenomenon agrees with the Arrhenius law [61]; higher temperature results in a higher conversion rate and consequently leading to higher CMEC yield. It can be concluded from the ANOVA Table 4 that the reaction temperature was found to be a highly influencing parameter on both the conversion of ECH and CMEC yield as evident from low p-value (< 0.0001).

5.3. Interactive effect of temperature and catalyst loading

The overall CMEC yield has been significantly influenced by the interaction between the catalyst loading and reaction temperature while CO_2 pressure and time have been kept at optimum values of 11 bar and 12 h respectively. For example, Figure.11 shows that at lower catalyst loading of 5% (w/w), only 34% of CMEC yield was recorded as a result of low ECH conversion at low catalyst loading. The CMEC yield increased steadily up to 68% as reaction temperature increased at moderate levels of catalyst loading from 333 K to 353 K. This phenomenon could be attributed to the increase in the catalyst surface area, which provides more contact area between the limiting reactant ECH and the active sites of the catalyst. Higher catalyst loading gives higher ECH conversion resulting in higher CMEC yield, an effect which is more pronounced at higher temperatures. However, at higher temperature above 353 K, a marginal decrease in CMEC yield was observed, which may be due to catalyst deactivation at very high temperature [10]. The contour plot in Figure 12b with elliptical shape demonstrated the significant and combine effect of the catalyst loading and reaction temperature. The result has also supported lower p-value (0.0005) of the interaction x_1x_3 term. As shown in Figure 12a, at any designated value of reaction temperature from 333 K to 353 K, the CMEC increased proportionally with catalyst loading. This observation was also supported by low p-value (< 0.0001).

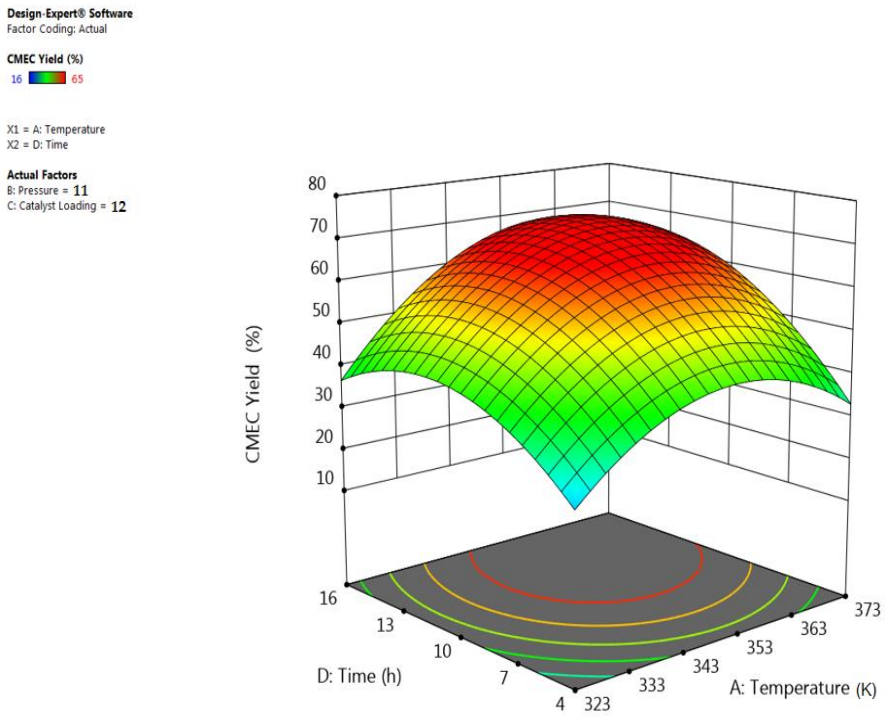

490

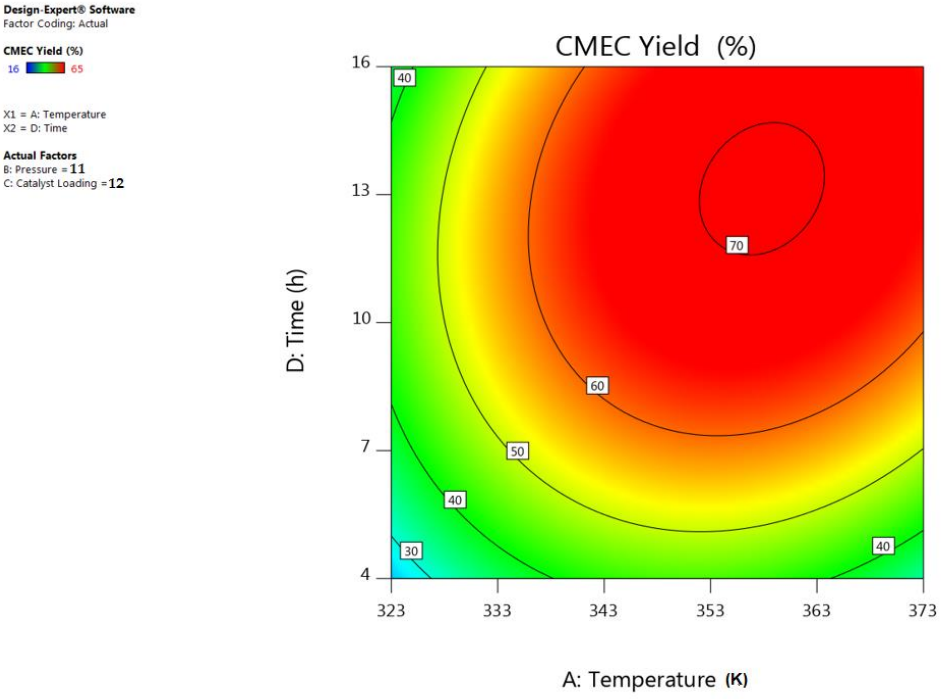

491

492

493 **Figure. 11.** (a) 3D response surface and (b) contour plot of reaction temperature and time *versus*

494 CMEC yield

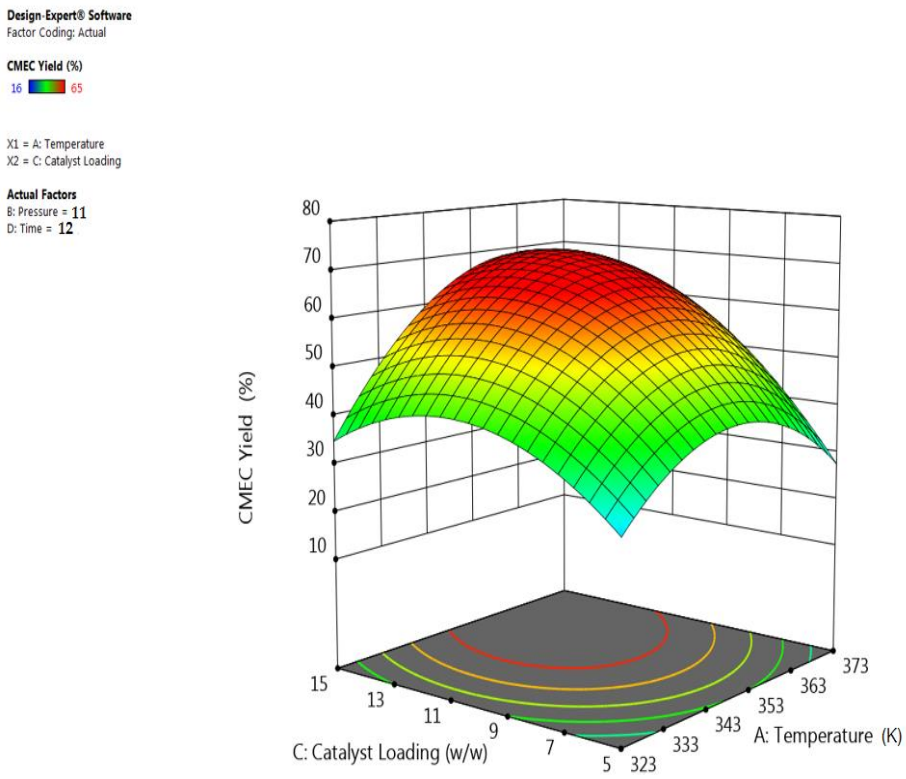

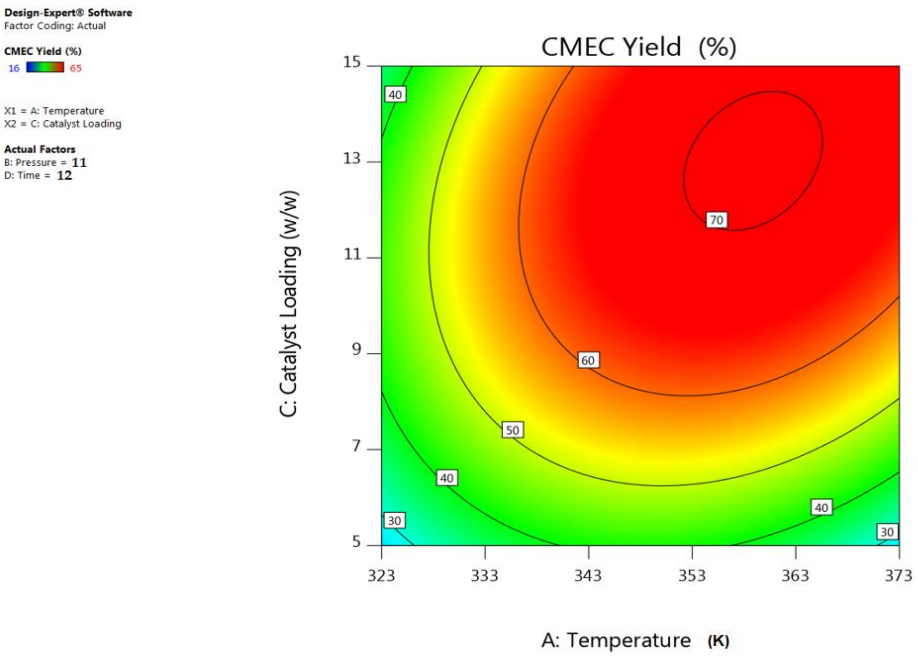

Figure. 12. 3D response surface and contour plot of reaction temperature and catalyst loading *versus* CMEC yield.

5.4. Interactive effect of time and pressure

Similar to the previous observation of the interaction effect of temperature and pressure, Figure. 13 demonstrates the interaction effect of CO_2 pressure and time on CMEC yield while maintaining reaction temperature and catalyst loading at 353 K and 12 %(w/w) respectively. For example, at a shorter reaction time of 4 h, there was a negligible effect of CO_2 pressure in the CMEC yield. Figure 13a shows that optimum reaction time of 12 h was observed at a CO_2 pressure of about 12 bar with a 68% of CMEC yield. It has been observed in Figure 13 that the CMEC yield reached a maximum at a reaction time of 12 h, thereafter, it was stable. A further increase in reaction time beyond this value caused a sharp drop in CMEC yield as indicated in surface plot of Figure 13b.

5.5. Interactive effect of time and catalyst loading

The contour and 3D surface plots in Figure 14 show the interaction effect between the reaction time and the catalyst loading at a constant temperature of 353 K and CO_2 pressure of 12 bar. The contour plots show less curvature up to 7 h of reaction time, which implied less influence of catalyst loading on CMEC yield between the reaction time of 2 to 6 h. However, a maximum CMEC yield of 68% was achieved at higher catalyst loading and reaction time of 12 % (w/w) and 12 h respectively. A declining effect was observed in Figure 14a as the catalyst loading goes above 12% (w/w). This reflects that the optimum catalyst loading had been exceeded. A similar trend was reported by Onyenkeadi et al. [9] on declining effect of catalyst loading beyond the optimum reaction time. Increase in the amount of catalyst loading can increase the number of active sites on the catalyst surface, and consequently, increases number of radicals (see S1). However, excessive increase of catalyst concentration beyond the optimum reaction time can result in a catalyst deactivation [8]. This phenomenon is totally in agreement with the recent reports of Feilizadeh et al. [62]

5.6. Interactive effect of catalyst loading and pressure

The exponential interaction effect between catalyst loading and pressure at a constant reaction time of 12 h and a temperature of 353 K is presented in Figure 15. However, the interaction produced a different effect on CMEC yield at different levels of interaction (i.e. different levels of interaction produce different effect on the ECH conversion). For example, Figure 15 shows that at the start of the reaction, 5 % (w/w) of catalyst loading at 7 bar of CO_2 pressure produced an increasing effect on the CMEC yield. As the catalyst loading was further increased from 5% to 10% (w/w), the CMEC yield was observed to increase steadily from 40% to 68% corresponding to an increase in CO_2 pressure from 7 to 11 bar. The CMEC yield was highest (68%) at a maximum catalyst loading of 12 % (w/w), when the CO_2 pressure was maintained at 11 bar as shown in Figure 15. However, a negative effect of excessive increase in CO_2 pressure was observed on CMEC yield (a drop to 64%) at this level of interaction between catalyst loading and pressure. This phenomenon can be attributed to catalyst deactivation at increased CO_2 pressure beyond the optimum. A similar experience was reported earlier by Zhang et al. [63]. The group have recorded a higher propylene carbonate (PC) yield with a fixed amount of immobilized ionic liquid/$ZnCl_2$ at a CO_2 pressure of 1.5 Mpa, however, a lower PC yield was observed at a higher CO_2 pressure of 2 MPa. Furthermore, they claimed that this phenomenon occurs when acidic CO_2 dissolves in basic epoxide to form a liquefied CO_2–epoxide complex, thereby inducing catalyst deactivation.

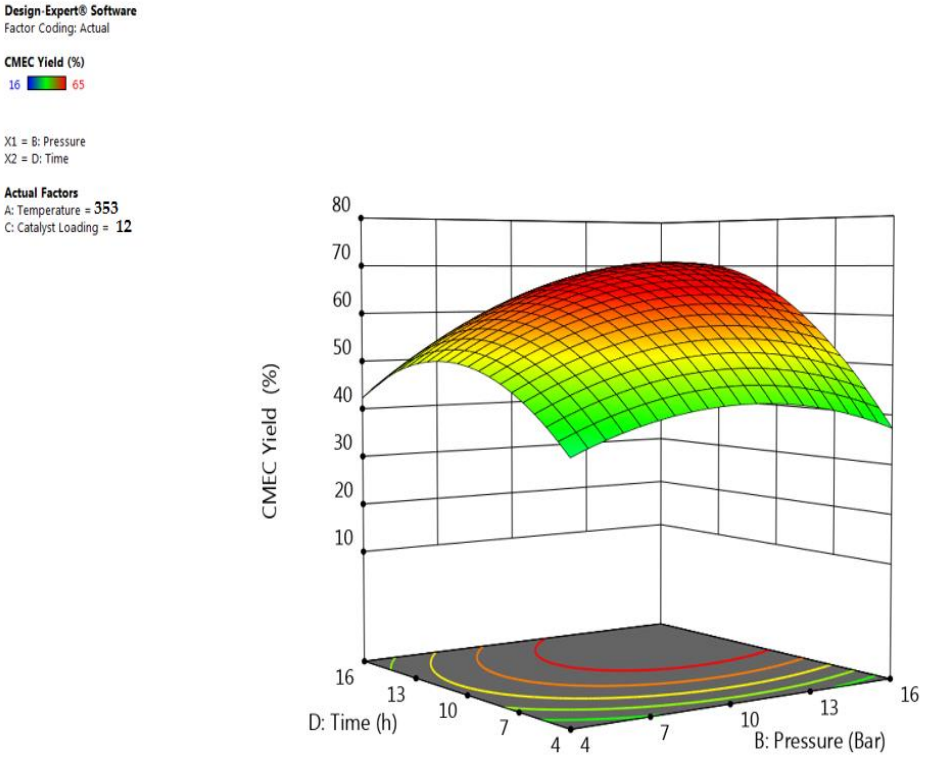

550
551

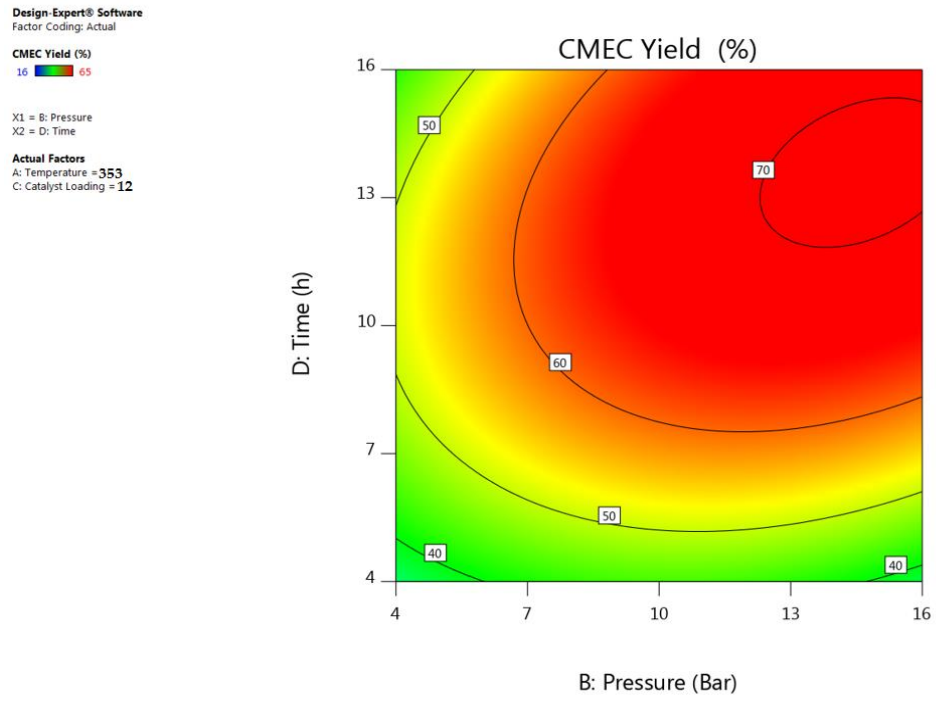

552
553 **Figure.13**. 3D response surface and contour plot of reaction time and pressure *versus* CMEC yield.

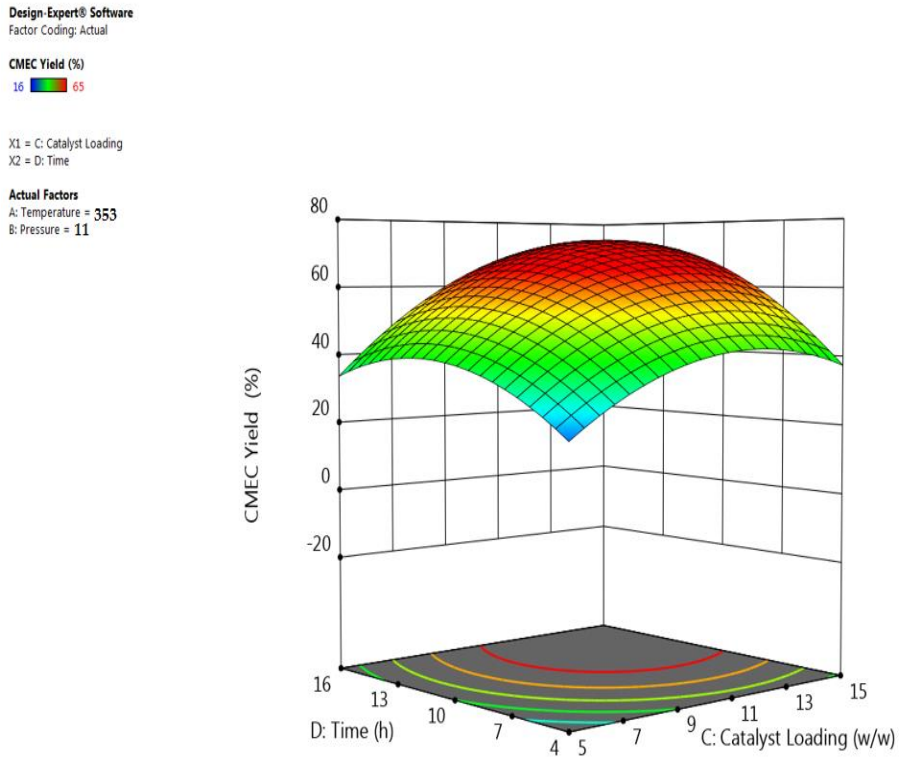

554

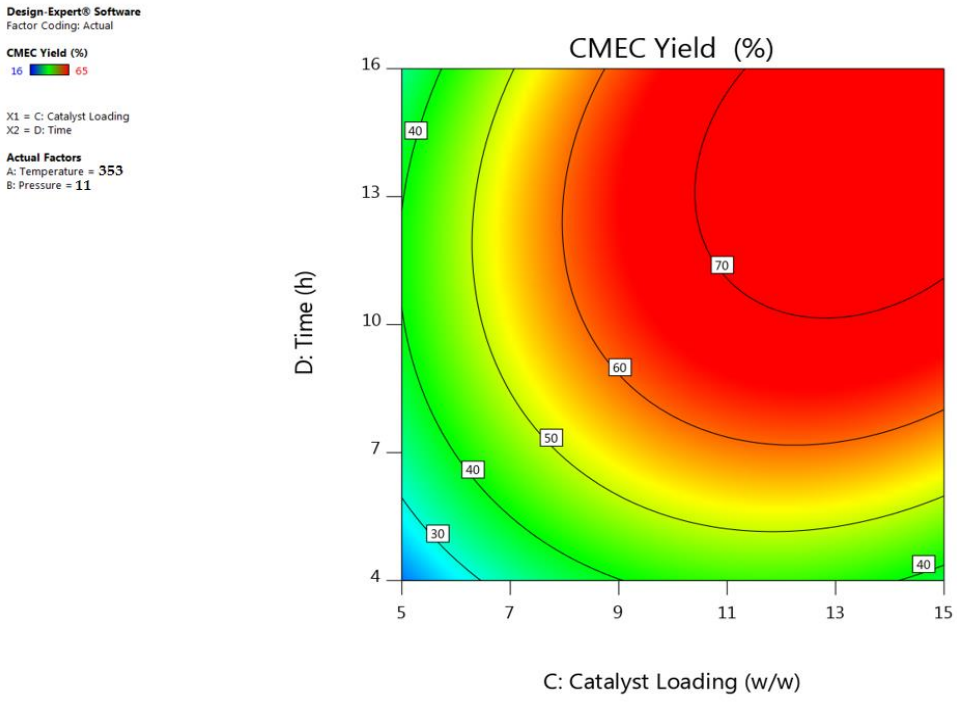

555

556 **Figure.14**. 3D response surface and contour plot of reaction time and catalyst loading *versus* CMEC
557 yield.

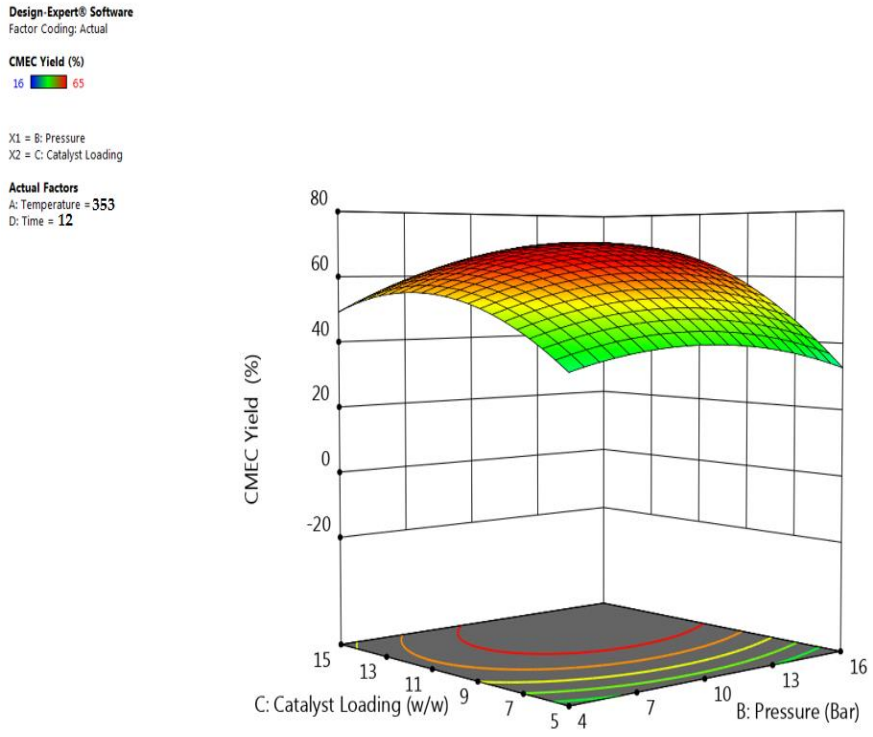

558

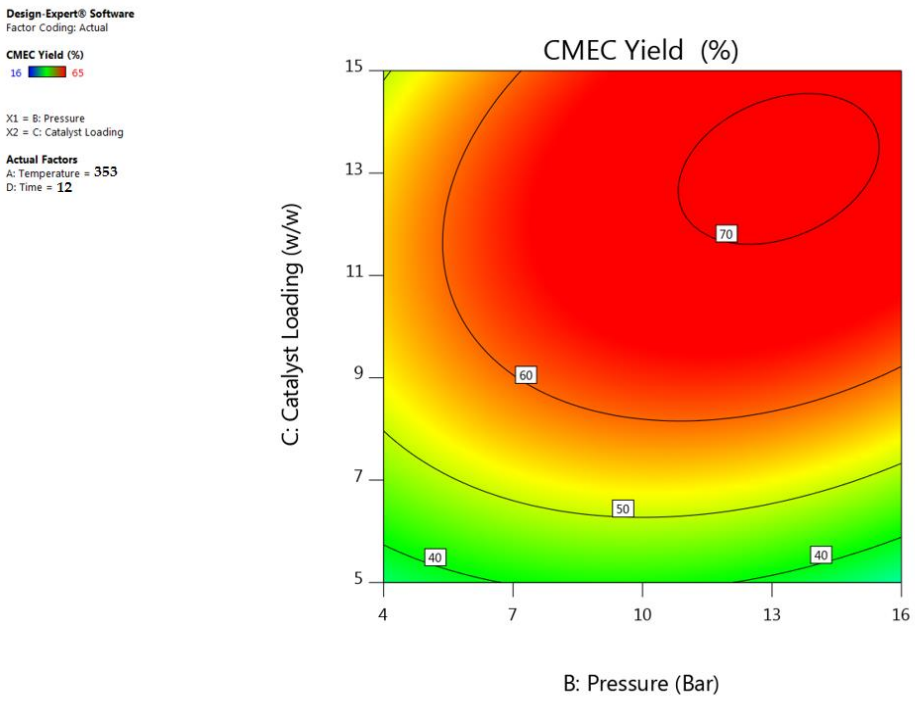

559

560 **Figure.15**. 3D response surface and contour plot of reaction pressure and catalyst loading *versus*
561 CMEC yield

562

563

564

6. Multiobjective Process Optimisation

The growing quest for greener substitute for fossil fuel has led to increased production, process optimisation and application of organic carbonate. As a result, the use of RSM has received more attention over conventional optimisation methods in order to investigate process optimum conditions and the interactive relationships between effective working variables. Although, finding the optimal reaction parameters for a single response using RSM is relatively simple; however, the optimisation of several responses at the same time is not an easy matter. Therefore, the optimisation targets for this study have been set to maximise the process productivity. Targets for both ECH conversion and CMEC yield have been set to reach the maximum values while both the reaction temperature and time have been targeted to minimum values with a viewpoint of reducing production cost at a maximum economic gain. Because of the catalyst efficiency and stability at optimum conditions, as a results, no specific target has been set for catalyst loading .

Based on the models generated and the accuracy between the actual experimental and predicted results, it can be construed that model shows high consistencies between the two results where the relative errors of the predicted results from the experimental data are 1.55% and 1.54% for ECH conversion and CMEC yield, respectively. The similarity between the predicted and experimental results at the optimum conditions has validated the predicted optimum conditions. The experimental results concluded that increase in reaction parameters increases ECH conversion and CMEC yield being 93% and 68% respectively.

Table 5. Optimisation constraints used to predict optimum conditions for chloromethyl ethylene carbonate synthesis

Factor	Code	Goal	Limits	
			Lower	Upper
Temperature (K	x_1	Minimise	313	373
Pressure (bar)	x_2	In range	2	16
Catalyst loading (%)	x_3	In range	5	15
Time (h)	x_4	Minimise	2	16
ECH conversion	Y_1	Maximise	60	93
CMEC yield	Y_2	Maximise	30	68

7. Catalyst Reusability Studies

In view of large scale industrial applications and to minimise production cost, the reusability studies of Zr/ZIF-8 catalyst has been investigated. The catalyst reusability process has also followed strict eco-regulation after all the predicted optimum parameters have been derived from BBD of RSM. The experiments were carried out in a high-pressure reactor at optimum reaction conditions, at 353 K, 11 bar with fresh 12% (w/w) ZIF-8 catalyst loading, for 12 h and at a stirring speed of 350 rpm. The catalyst after Run 1 in the cycloaddition reaction was washed with ethanol and acetone, centrifuged, and oven dried at 343 K for 12 h before reuse. The recovered catalysts were reused for up to 7 subsequent experiments as shown in Figure 16 following the same experimental procedure. The catalyst exhibited no loss of activity indicating the catalyst stability for cycloaddition reaction of CO_2 epichlorohydrin. Incorporating zirconium into ZIF-8 has significantly increased the catalytic performance of Zr/ZIF-8 with the conversion of ECH and the yield of CMEC being 93%, and 68% respectively. The activity of reused Zr/ZIF-8 catalyst showed consistent stability over seven subsequent runs as indicated in Figure 16. Although, a very slight decrease in the yield of CMEC

from 68% (fresh) to 67% (recycled) was observed in the seventh run. Carbonaceous material formed during the reaction may explain in part the lower activity of the recycled catalysts [64].

Although, the difference in the error bars status between the ECH conversion and CMEC yield may be statistically significant, this may be attributed to the formation of some side products associated with the coupling reaction of CO_2 and ECH. The following side products have been identified by the GC analysis; 3-chloropropane 1,2-diol and 2,5-bis (chloromethyl)-1,4-dioxane.

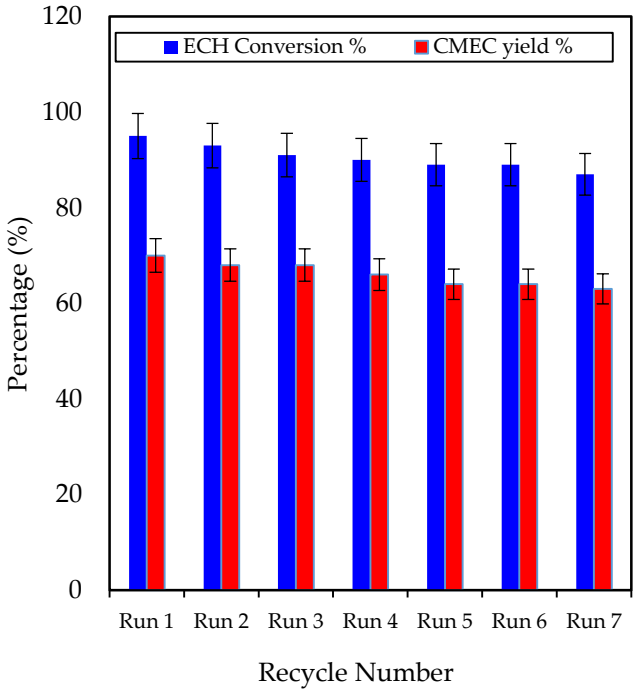

Figure 16. Catalyst reusability studies of Zr/ZIF-8 on conversion of ECH, and CMEC yield using predicted response surface methodology's optimum condition of catalyst loading 12% (w/w); reaction temperature 353 K; CO_2 pressure 11 bar, reaction time 12 h, stirring speed 350 rpm.

8. Conclusions

In this study, Zr/ZIF-8 catalyst has been successfully used for process optimisation in the synthesis of CMEC using RSM. In total, 29 run of experiments were conducted for optimum design and modelling. The developed model was validated to assess the agreement between its predictions and a set of experimental data. The development of a novel Zr/ZIF-8 catalyst *via* a simple low cost solvothermal method has demonstrated that the catalyst is viable for large-scale industrial applications. The catalyst has shown a good substrate tolerance as demonstrated by its activity towards epichlorohydrin. More importantly, the reaction has been carried out under solvent free and co-catalyst free conditions. The heterogeneity of the catalyst has been proven by recovering and reusing the catalyst for up to seven times without any significant loss in catalytic activity. Furthermore, PXRD, FT-IR, and TGA analysis (see supplementary information sheets) of the recycled catalyst shows that the catalyst framework is quite stable after recycled experiments. The high selectivity towards epichlorohydrin carbonate, simple separation of catalyst by centrifugation and excellent recyclability demonstrated that the catalyst is viable for industrial applications. We believe

that this work could provide a new direction for designing more sustainable heterogeneous catalysts for greener synthesis of organic carbonates *via* CO_2 utilisation.

Acknowledgements

Bisi Olaniyan is immensely grateful to the School of Engineering, LSBU, UK for partial financial assistance throughout this research work.

References

1. Miao, C.-X.; Wang, J.-Q.; He, L.-N. Catalytic Processes for Chemical Conversion of Carbon Dioxide into Cyclic Carbonates and Polycarbonates. *Open Org. Chem. J.* **2008**, *2*, 68–82.
2. Liu, B.; Liu, M.; Liang, L.; Sun, J. Guanidine Hydrochloride/ZnI2 as Heterogeneous Catalyst for Conversion of CO_2 and Epoxides to Cyclic Carbonates under Mild Conditions. *Catalysts* **2015**, *5*, 119–130.
3. Xie, Y.; Wang, T.-T.; Liu, X.-H.; Zou, K.; Deng, W.-Q. Capture and conversion of CO_2 at ambient conditions by a conjugated microporous polymer. *Nat. Commun.* **2013**, *4*, 1960–1967.
4. North, M.; Pasquale, R.; Young, C. Synthesis of cyclic carbonates from epoxides and CO_2. *Green Chem.* **2010**, *12*, 1514–1539.
5. Sathe, A.A.; Nambiar, A.M.; Sturgis, N.; Rioux, M. Synthesis of cyclic organic carbonates via catalytic oxidative carboxylation of olefins in flow reactors. *Catal. Sci. Technol.* **2017**, *7*, 2–3.
6. Liu, A.-H.; Li, Y.-N.; He, L.-N. Organic synthesis using carbon dioxide as phosgene-free carbonyl reagent. *Pure Appl. Chem.* **2012**, *84*, 581–602.
7. Maeda, C.; Miyazaki, Y.; Ema, T. Recent progress in catalytic conversions of carbon dioxide. *Catal. Sci. Technol.* **2014**, *4*, 1482.
8. Adeleye, A.I.; Kellici, S.; Heil, T.; Morgan, D.; Vickers, M.; Saha, B. Greener synthesis of propylene carbonate using graphene-inorganic nanocomposite catalysts. *Catal. Today* **2015**, *256*, 347–357.
9. Onyenkeadi, V.; Kellici, S.; Saha, B. Greener synthesis of 1,2-butylene carbonate from CO_2 using graphene-inorganic nanocomposite catalyst. *Energy* **2018**, *165*, 867–876.
10. Adeleye, A.I.; Patel, D.; Niyogi, D.; Saha, B. Efficient and greener synthesis of propylene carbonate from carbon dioxide and propylene oxide. *Ind. Eng. Chem. Res.* **2014**, *53*, 18647–18657.
11. Sakakura, T.; Kohno, K. The synthesis of organic carbonates from carbon dioxide. *Chem. Commun.* **2009**, 1312–1330.
12. Shukla, K.; Srivastava, V.C. Synthesis of organic carbonates from alcoholysis of urea: A review. *Catal. Rev. - Sci. Eng.* **2017**, *59*, 1–43.
13. Dalpozzo, R.; Ca, N. Della; Gabriele, B.; Mancuso, R. Recent advances in the chemical fixation of carbon dioxide: A green route to carbonylated heterocycle synthesis. *Catalysts* **2019**, *9* 6198–6202.
14. Lu, X.B.; Liang, B.; Zhang, Y.J.; Tian, Y.Z.; Wang, Y.M.; Bai, C.X.; Wang, H.; Zhang, R. Asymmetric Catalysis with CO_2: Direct Synthesis of Optically Active Propylene Carbonate from Racemic Epoxides. *J. Am. Chem. Soc.* **2004**, *126*, 3732–3733.
15. Paddock, R.L.; Nguyen, S.T. Chemical CO_2 fixation: CR(III) salen complexes as highly efficient catalysts for the coupling of CO_2 and epoxides. *J. Am. Chem. Soc.* **2001**, *123*, 11498–

11499.
16. Caló, V.; Nacci, A.; Monopoli, A.; Fanizzi, A. Cyclic carbonate formation from carbon dioxide and oxiranes in tetrabutylammonium halides as solvents and catalysts. *Org. Lett.* **2002**, *4*, 2561–2563.
17. He, Q.; O'Brien, J.W.; Kitselman, K.A.; Tompkins, L.E.; Curtis, G.C.T.; Kerton, F.M. Synthesis of cyclic carbonates from CO_2 and epoxides using ionic liquids and related catalysts including choline chloride-metal halide mixtures. *Catal. Sci. Technol.* **2014**, *4*, 1513–1528.
18. Kihara, N.; Hara, N.; Endo, T. Catalytic Activity of Various Salts in the Reaction of 2,3-Epoxypropyl Phenyl Ether and Carbon Dioxide under Atmospheric Pressure. *J. Org. Chem.* **1993**, *58*, 6198–6202.
19. Castro-Osma, J.A.; Lamb, K.J.; North, M. Cr(salophen) Complex Catalyzed Cyclic Carbonate Synthesis at Ambient Temperature and Pressure. *ACS Catal.* **2016**, *6*, 5012–5025.
20. Rulev, Y.A.; Larionov, V.A.; Lokutova, A. V.; Moskalenko, M.A.; Lependina, O.L.; Maleev, V.I.; North, M.; Belokon, Y.N. Chiral Cobalt(III) Complexes as Bifunctional Brønsted Acid-Lewis Base Catalysts for the Preparation of Cyclic Organic Carbonates. *ChemSusChem* **2016**, *9*, 216–222.
21. Jutz, F.; Grunwaldt, J.D.; Baiker, A. Mn(III)(salen)-catalyzed synthesis of cyclic organic carbonates from propylene and styrene oxide in 'supercritical' CO_2. *J. Mol. Catal. A Chem.* **2008**, *279*, 94–103.
22. Kuznetsova, S.A.; Rulev, Y.A.; Larionov, V.A.; Smol'yakov, A.F.; Zubavichus, Y. V.; Maleev, V.I.; Li, H.; North, M.; Saghyan, A.S.; Belokon, Y.N. Self-Assembled Ionic Composites of Negatively Charged Zn(salen) Complexes and Triphenylmethane Derived Polycations as Recyclable Catalysts for the Addition of Carbon Dioxide to Epoxides. *ChemCatChem* **2019**, *11*, 511–519.
23. Sakakura, T.; Kohno, K. The synthesis of organic carbonates from carbon dioxide. *Chem. Commun.* **2009**, 1312.
24. Luo, R.; Zhou, X. Metal- and solvent-free synthesis of cyclic carbonates from epoxides and CO_2 in the presence of graphite oxide and ionic liquid under mild conditions : A kinetic study. *Carbon N. Y.* **2014**, *82*, 1–11.
25. Siewniak, A.; Jasiak, K.; Baj, S. An efficient method for the synthesis of cyclic carbonates from CO_2 and epoxides using an effective two-component catalyst system: Polymer-supported quaternary onium salts and aqueous solutions of metal salts. *Appl. Catal. A Gen.* **2014**, *482*, 266–274.
26. Ma, D.; Li, B.; Liu, K.; Zhang, X.; Zou, W.; Yang, Y.; Li, G.; Shi, Z.; Feng, S. Bifunctional MOF heterogeneous catalysts based on the synergy of dual functional sites for efficient conversion of CO_2 under mild and co-catalyst free conditions. *J. Mater. Chem. A* **2015**, *3*, 23136–23142.
27. Saada, R.; AboElazayem, O.; Kellici, S.; Heil, T.; Morgan, D.; Lampronti, G.I.; Saha, B. Greener synthesis of dimethyl carbonate using a novel tin-zirconia/graphene nanocomposite catalyst. *Appl. Catal. B Environ.* **2018**, *226*, 451–462.
28. Saptal, V.B.; Bhanage, B.M. Current advances in heterogeneous catalysts for the synthesis of cyclic carbonates from carbon dioxide. *Curr. Opin. Green Sustain. Chem.* **2017**, *3*, 1–10.
29. Adeleye, A. I. (Supervisor-Saha. B) Heterogeneous Catalytic Conversion of Carbon Dioxide to Value Added Chemicals. PhD Thesis, *London South Bank University*, London UK. June, **2015**.

30. Cyclic carbonates synthesis from epoxides and CO_2 over metal–organic framework Cr-MIL-101. *J. Catal.* **2013**, *298*, 179–185.
31. Zalomaeva, O. V.; Chibiryaev, A.M.; Kovalenko, K.A.; Kholdeeva, O.A.; Balzhinimaev, B.S.; Fedin, V.P. Cyclic carbonates synthesis from epoxides and CO_2 over metal-organic framework Cr-MIL-101. *J. Catal.* **2013**, *298*, 179–185.
32. Beyzavi, M.H.; Stephenson, C.J.; Liu, Y.; Karagiaridi, O.; Hupp, J.T.; Farha, O.K. Metalâ€"Organic Framework-Based Catalysts: Chemical Fixation of CO_2 with Epoxides Leading to Cyclic Organic Carbonates. *Front. Energy Res.* **2015**, *2*, 1–10.
33. Jumbri, K.; Al-Haniff Rozy, M.F.; Ashari, S.E.; Mohamad, R.; Basri, M.; Fard Masoumi, H.R. Optimisation and characterisation of lipase catalysed synthesis of a kojic monooleate ester in a solvent-free system by response surface methodology. *PLoS One* **2015**, *10*, 1–13.
34. JK, K.; MJ, M.; JK, K. Response Surface Methodology Approach to the Optimization of Potato (Solanum tuberosum) Tuber Yield Using Second-Order Rotatable Design. *J. Biom. Biostat.* **2017**, *08*.
35. Manohar, M.; Joseph, J.; Selvaraj, T.; Sivakumar, D. Application of box Behnken design to optimize the parameters for turning inconel 718 using coated carbide tools. *Int. J. Sci. Eng. Res.* **2013**, *4*, 620–642.
36. Onyenkeadi, V.; Aboelazayem, O.; Saha, B. Systematic multivariate optimisation of butylene carbonate synthesis via CO_2 utilisation using graphene-inorganic nanocomposite catalysts. *Catal. Today* **2019**, 1–13.
37. Aboelazayem, O.; El-Gendy, N.S.; Abdel-Rehim, A.A.; Ashour, F.; Sadek, M.A. Biodiesel production from castor oil in Egypt: Process optimisation, kinetic study, diesel engine performance and exhaust emissions analysis. *Energy* **2018**, *157*, 843–852.
38. Jeirani, Z.; Mohamed Jan, B.; Si Ali, B.; Mohd. Noor, I.; Chun Hwa, S.; Saphanuchart, W. The optimal mixture design of experiments: Alternative method in optimizing the aqueous phase composition of a microemulsion. *Chemom. Intell. Lab. Syst.* **2012**, *112*, 1–7.
39. Sadeghi, N.; Sharifnia, S.; Do, T.O. Optimization and modeling of CO_2 photoconversion using a response surface methodology with porphyrin-based metal organic framework. *React. Kinet. Mech. Catal.* **2018**, *125*, 411–431.
40. Yu, X.L.; He, Y. Application of Box-Behnken designs in parameters optimization of differential pulse anodic stripping voltammetry for lead(II) determination in two electrolytes. *Sci. Rep.* **2017**, *7*, 1–8.
41. Kumar, A.; Gupta, M.; Mazumder, A.; Poluri, K.M.; Rao, V.K. Use of Box Behnken Design for Development of High Throughput Quantitative Proton Nuclear Magnetic Resonance Experiments for Industrial Applications. *Ind. Eng. Chem. Res.* **2017**, *56*, 2873–2882.
42. Schejn, A.; Aboulaich, A.; Balan, L.; Falk, V.; Lalevée, J.; Medjahdi, G.; Aranda, L.; Mozet, K.; Schneider, R. Cu^{2+} -doped zeolitic imidazolate frameworks (ZIF-8): efficient and stable catalysts for cycloadditions and condensation reactions. *Catal. Sci. Technol.* **2015**, *5*, 1829–1839.
43. Thi Thanh, M.; Vinh Thien, T.; Thi Thanh Chau, V.; Dinh Du, P.; Phi Hung, N.; Quang Khieu, D. Synthesis of Iron Doped Zeolite Imidazolate Framework-8 and Its Remazol Deep Black RGB Dye Adsorption Ability. *J. Chem.* **2017**, 8, 635–650.

762 44. Saada, R. Catalytic conversion of carbon dioxide (CO_2) into value added chemicals. **2015**.
763 45. Gallardo-Fuentes, S.; Contreras, R.; Isaacs, M.; Honores, J.; Quezada, D.; Landaeta, E.;
764 Ormazábal-Toledo, R. On the mechanism of CO_2 electro-cycloaddition to propylene oxides.
765 *J. CO_2 Util.* **2016**, *16*, 114–120.
766 46. Liu, Y.; Liu, F.; Ni, L.; Meng, M.; Meng, X.; Zhong, G.; Qiu, J. A modeling study by response
767 surface methodology (RSM) on Sr(II) ion dynamic adsorption optimization using a novel
768 magnetic ion imprinted polymer. *RSC Adv.* **2016**, *6*, 54679–54692.
769 47. Mäkelä, M. Experimental design and response surface methodology in energy applications:
770 A tutorial review. *Energy Convers. Manag.* **2017**, *151*, 630–640.
771 48. Zhu, Z.; Rosendahl, L.; Toor, S.S.; Chen, G. Optimizing the conditions for hydrothermal
772 liquefaction of barley straw for bio-crude oil production using response surface
773 methodology. *Sci. Total Environ.* **2018**, *630*, 560–569.
774 49. Lee, D.W.; Marasini, N.; Poudel, B.K.; Kim, J.H.; Cho, H.J.; Moon, B.K.; Choi, H.G.; Yong,
775 C.S.; Kim, J.O. Application of Box-Behnken design in the preparation and optimization of
776 fenofibrate-loaded self-microemulsifying drug delivery system (SMEDDS). *J. Microencapsul.*
777 **2014**, *31*, 31–40.
778 50. Long, X.; Cai, L.; Li, W. RSM-based assessment of pavement concrete mechanical properties
779 under joint action of corrosion, fatigue, and fiber content. *Constr. Build. Mater.* **2019**, *197*, 406–
780 420.
781 51. Rabiee, F.; Mahanpoor, K. Catalytic oxidation of SO_2 by novel Mn/copper slag nanocatalyst
782 and optimization by Box-Behnken design. *Int. J. Ind. Chem.* **2018**, *9*, 27–38.
783 52. Mohammadifard, H.; Amiri, M.C. On tailored synthesis of nano $CaCO_3$ particles in a
784 colloidal gas aphron system and evaluating their performance with response surface
785 methodology for heavy metals removal from aqueous solutions. *J. Water Environ.*
786 *Nanotechnol.* **2018**, *3*, 141–149.
787 53. Abhang, R.M.; Wani, K.S.; Patil, V.S. Synthesis and Characterization of ZIF-8 Filler for
788 preparation of Mixed Matrix Membrane. *International Journal of Scientific & Engineering*
789 *Research.* **2015**, *6*, 1276–1280.
790 54. Kilic, A.; Durgun, M.; Aytar, E.; Yavuz, R. Synthesis and characterization of novel positively
791 charged organocobaloximes as catalysts for the fi xation of CO_2 to cyclic carbonates. *J.*
792 *Organomet. Chem.* **2018**, *858*, 78–88.
793 55. Shi, J.; Song, J.; Ma, J.; Zhang, Z.; Fan, H.; Han, B. Effective synthesis of cyclic carbonates
794 from CO_2 and epoxides catalyzed by KI/cucurbit[6]uril. *Pure Appl. Chem.* **2013**, *85*, 1633–1641.
795 56. Zhong, S.; Liang, L.; Liu, B.; Sun, J. $ZnBr_2$/DMF as simple and highly active Lewis acid–base
796 catalysts for the cycloaddition of CO_2 to propylene oxide. *J. CO_2 Util.* **2014**, *6*, 75–79.
797 57. Xuan, K.; Pu, Y.; Li, F.; Li, A.; Luo, J.; Li, L.; Wang, F.; Zhao, N. Direct synthesis of dimethyl
798 carbonate from CO_2 and methanol over tri fl uoroacetic acid modulated UiO-66. *J. CO_2 Util.*
799 **2018**, *27*, 272–282.
800 58. Han, X.; Zhu, G.; Ding, Y.; Miao, Y.; Wang, K.; Zhang, H.; Wang, Y.; Liu, S. Bin Selective
801 catalytic synthesis of glycerol monolaurate over silica gel-based sulfonic acid functionalized
802 ionic liquid catalysts. *Chem. Eng. J.* **2019**, *359*, 733–745.
803 59. Bahrami, M.; Amiri, M.J.; Bagheri, F. Optimization of the lead removal from aqueous
804 solution using two starch based adsorbents: Design of experiments using response surface

methodology (RSM). *J. Environ. Chem. Eng.* **2019**, *7*, 102793.
60. Nandiwale, K.Y.; Bokade, V. V. Process optimization by response surface methodology and kinetic modeling for synthesis of methyl oleate biodiesel over H3PW12O40 anchored montmorillonite K10. *Ind. Eng. Chem. Res.* **2014**, *53*, 18690–18698.
61. Peng, J.; Wang, S.; Yang, H.; Ban, B.; Wei, Z.; Wang, L.; Lei, B. Highly e ffi cient fi xation of carbon dioxide to cyclic carbonates with new multi-hydroxyl bis- (quaternary ammonium) ionic liquids as metal-free catalysts under mild conditions. *Fuel* **2018**, *224*, 481–488.
62. Feilizadeh, M.; Rahimi, M.; Zakeri, S.M.E.; Mahinpey, N.; Vossoughi, M.; Qanbarzadeh, M. Individual and interaction effects of operating parameters on the photocatalytic degradation under visible light illumination: Response surface methodological approach. *Can. J. Chem. Eng.* **2017**, *95*, 1228–1235.
63. Zhang, Y.; Yin, S.; Luo, S.; Au, C.T. Cycloaddition of CO_2 to epoxides catalyzed by carboxyl-functionalized imidazolium-based ionic liquid grafted onto cross-linked polymer. *Ind. Eng. Chem. Res.* **2012**, *51*, 3951–3957.
64. Bosch, M.; Zhang, M.; Zhou, H.-C. Increasing the Stability of Metal-Organic Frameworks. *Adv. Chem.* **2014**, *2014*, 1–8.